약학박사 학위논문

Study on Factors Limiting Intestinal Drug Absorption: Contribution of interplay between metabolism and efflux transport in intestinal epithelial cells, and intestinal stability on the absorption

약물의 장관흡수를 제한하는 요소에 관한 연구: 장관 상피세포 내 대사-배출 수송의 interplay 및 장관 내 안정성이 흡수에 미치는 영향

2017년 2월

서울대학교 대학원

약학과 약제과학 전공

유 헌 민

ABSTRACT

Study on Factors Limiting Intestinal Drug Absorption: Contribution of interplay between metabolism and efflux transport in intestinal epithelial cells, and intestinal stability on the absorption

Heon-Min Ryu

Department of Pharmaceutical Science

College of Pharmacy

The Graduate School

Seoul National University

PART I. Enhanced intestinal absorption of indinavir and its metabolic conversion to M6 by the co-administration of HM-30181A, a P-glycoprotein inhibitor

Intestinal P-glycoprotein (P-gp), an efflux transporter, may render its substrate to 'recycle' during the intestinal absorption process. The objective of this study is to determine the contribution of P-gp mediated 'recycling' in the intestinal first pass metabolism. To examine whether HM-30181A, a

potentially specific inhibitor for P-gp, interacted with CYP enzymes (i.e., 1A2, 2C9, 2C19, 2D6, 3A4), the metabolic stability of standard substrates for major CYP enzymes in rat liver microsomes was studied in the presence and the absence HM-30181A. Furthermore, to determine whether compound interacted with typical SLC transporters (i.e., rOatp1b2, rOat1, rOat3 and rOct2), the uptake of their standard substrates in MDCKII/FRT cells expressing the transporters was studied with or without the compound. In this study, indinavir was selected as the model compound since the drug is a well-established substrate for both P-gp and CYP3A4. Rats orally received the dose of 10 mg/kg of HM-30181A, 10 minutes prior to the indinavir administration (10 mg/kg orally). For portal vein infusion study, rats received indinavir infusion via portal vein catheter at the rate of 15 mg/kg/h for 20 min while the inhibitor was given orally 10 min prior to the initiation of the infusion. It was found that HM-30181A did not affect the activity of typical CYP enzymes (1A2, 2C9, 2C19, 2D6 or 3A4) and SLC transporters (rOatp1b2, rOat1, rOat3, rOct2) suggesting that the compound was a specific inhibitor for P-gp. In oral administration study, C_{max} values of indinavir ($C_{max,\ IND}$) for control and HM30181-treated group were (in mean ± SD) 0.614 ± 0.083 and 1.51 ± 0.64 μg/mL, respectively. AUC values for indinavir (AUC_{IND}) of the two groups were also affected similarly [viz, in HM-30181 treated group, AUC approximately 111% higher ($p<0.05$) than control group]. AUC of M6 (AUC_{M6}) was increased in HM-30181A-treated group to the similar extent of the increase found with AUC_{IND}. For the case of portal vein infusion

study, $C_{max, IND}$, AUC_{IND} and AUC_{M6} were 1.4, 2.5 and 1.9-fold increased when HM-30181A was co-administered. In Ussing chamber study, Papp values were 2.85 ± 0.19 and 4.34 ± 1.08 X 10^{-6} cm/sec for untreated and HM-30181A treated group, respectively. Amount of indinavir was tend to increase (2650 ± 1130 and 3290 ± 1110 pmole/g tissue, respectively), although the values were not statistically different. For the case of M6 conversion, the amount of the metabolite was increased (54.9 ± 10.9 and 77.3 ± 16.3 pmole/g tissue, respectively, $p < 0.05$) in the intestine when the tissue was treated with HM-30181A, consistent with a simulation result with a kinetic model assuming cooperative action of recycling and metabolism. Therefore, the in vivo observations with different routes of indinavir administration, ex vivo study and in silico study collectively showed that the absorption and metabolism of indinavir is slightly enhanced by HM-30181A.

PART II. Quantification of EC-18, a synthetic monoacetyldiglyceride (1-palmitoyl-2-linoleoyl-3-acetyl-rac-glycerol), in rat and mouse plasma by liquid-chromatography/tandem mass spectrometry

EC-18 (i.e., 1-palmitoyl-2-linoleoyl-3-acetyl-rac-glycerol), an active ingredient in Rockpid®, has been reported to be useful in controlling various types of inflammations, particularly those caused by neutropenia. Although this product was originally approved as a functional food in Korea, it is

currently in phase II clinical trials for use in managing the severe chemotherapy-induced neutropenia in patients with advanced breast cancer who are receiving intermediate febrile neutropenia risk chemotherapy. The objective of this study was to develop a rapid, sensitive method for the determination of EC-18 in rat and mouse plasma and to evaluate the applicability of the assay in pharmacokinetic studies. EC-18 was extracted with MeOH from rat and mouse plasma samples, and the extract directly introduced onto an LC-MS/MS system. The analyte and EC-18-d3, an internal standard, were analyzed by multiple reaction monitoring (MRM) at m/z transitions of 635.4→355.4 for EC-18 and 638.4→338.4 for the internal standard, respectively. The lower limit of quantification (LLOQ) was determined at 50 ng/mL, with an acceptable linearity in the range from 50 to 10000 ng/mL ($r > 0.999$) for both matrices. Validation parameters such as accuracy, precision, dilution, recovery, matrix effects and stability were found to be within the acceptance criteria of the assay validation guidelines, indicating that the assay is applicable for estimating EC-18 in concentrations in the range examined. EC-18 was readily determined in plasma samples for periods of up to 8 h following an intravenous bolus injection of 1 mg/kg in rats and at 5 mg/kg in mice, respectively, and up to 24 h following the oral administration of 2000 mg/kg in mice. The findings indicate that the current analytical method is applicable for pharmacokinetic studies of EC-18 in small animals.

Keywords: Intestinal P-glycoprotein; Intestinal first pass metabolism; P-gp recycling; Indinavir; HM-30181A; EC-18; 1-palmitoyl-2-linoleoyl-3-acetyl-rac-glycerol; Pharmacokinetics; LC-MS/MS

Student Number: 2010-21709

CONTENTS

PART II. Quantification of EC-18, a synthetic monoacetyldiglyceride (1-palmitoyl-2-linoleoyl-3-acetyl-rac-glycerol), in rat and mouse plasma by liquid-chromatography/tandem mass spectrometry

LIST OF TABLES

PART I. Enhanced intestinal absorption of indinavir and its metabolic conversion to M6 by the co-administration of HM-30181A, a P-glycoprotein inhibitor

PART II. Quantification of EC-18, a synthetic monoacetyldiglyceride (1-palmitoyl-2-linoleoyl-3-acetyl-rac-glycerol), in rat and mouse plasma by liquid-chromatography/tandem mass spectrometry

LIST OF FIGURES

PART I. Enhanced intestinal absorption of indinavir and its metabolic conversion to M6 by the co-administration of HM-30181A, a P-glycoprotein inhibitor

PART II. Quantification of EC-18, a synthetic

INTRODUCTION

Oral administration of drugs is probably the most popular way of administration because of its convenience, economy and relative safety. Despite these advantages, however, complications, such as inadequate solubility of active ingredient in gastric/intestinal fluids and instability in the intestine do exist so that, in some cases, the rate and extent intestinal absorption be altered/limited significantly (Higuchi et al., 1981; Ho et al., 1983). In addition to these complications, various biological / physiochemical factors such as food, gastric and intestinal transit time, membrane permeability, intestinal pH and mesenteric blood flow rate may affect its intestinal absorption (Benet et al., 1996). As an example of the complexity of intestinal absorption of drugs, it is well known that the absorption of tetracycline hydrochloride was significantly decreased with iron, milk or food in healthy volunteer (Leyden, 1985). In addition, the bioavailability of celecoxib was much higher when given as a solution compared with a capsule (Paulson et al., 2001), indicating that the physical form of the formulation also affects the intestinal absorption.

One of the most widely recognized problems in the intestinal drug absorption is pre-systemic first pass effect in the intestine and/or in the liver (Thummel et al., 1997; Lin et al., 1999a): Metabolism during the transport across the intestinal epithelium and through the liver may occur so that the amount of drug reaching the systemic circulation may be comparatively less.

As examples to the importance of pre-systemic elimination, baicalein and metoprolol, compounds having adequate permeability across the small intestine, had low bioavailability due to hepatic first pass effect (Zhang et al., 2005; Yoon et al., 2011). In addition to the metabolic enzymes affecting the extent of absorption, drug transporters may be involved in intestinal absorption of some drugs. During 1990s', the molecular characteristics of drug transporters from animals and humans has been extensively studied (Elferink et al., 1995; Meijer et al., 1997; Müller and Jansen, 1998; Kim et al., 2000): From these studies, it is now well recognized that not only the physicochemical properties but also the affinity toward drug transporter(s) may be a factor in the intestinal absorption for certain drugs. For added complexity in understanding drug absorption in the intestine, efflux transporters [e.g., MDRs and MRPs; (Kool et al., 1997; Watkins, 1997)] that pump their substrates back into the lumen are reported be expressed in the intestine, in addition to the influx transporters [e.g., OATs, OATPs and OCTs (Koepsell, 1998; Sekine et al., 1999; Tamai et al., 2000); transporters that enhances the intestinal drug absorption]. For example, exposure of rosuvastatin (an OATP2B1 substrate) was approximately markedly decreased with ronacaleret (an OATP2B1 inhibitor) (Johnson et al., 2016), suggesting importance of transporters in the intestinal absorption of certain drugs. In addition, the intestinal absorption of cyclosporine A (an MDR1 substrate) was significantly increased in MDR1 gene knockout mouse (Lee et al., 2005). Amongst these, P-glycoprotein (MDR1) is one of the most extensively studied

efflux transporters. This ATP-binding cassette transporter is reported to be expressed in the apical membrane of the villus tip of gut enterocyte, and transports the substrate back to the luminal side (Watkins, 1997). Interestingly, although it is still highly controversial, the concerted action of the efflux transporter and the drug metabolizing enzyme was reported so that the absorption time may be prolonged by the action of the efflux transporter thereby leading to an enhanced chance for metabolic reaction (Johnson et al., 2001; Cummins et al., 2002; Cummins et al., 2003). On the contrary, however, in/ex vivo studies, along with theoretical analysis, seems to suggested a decreased metabolism for the dual substrates by the involvement of P-gp in the intestine. (Lan et al., 2000; Tam et al., 2003). In part I of this thesis, the interplay between P-glycoprotein and CYP3A4 was studied with indinavir, a common substrate for the transporter and the enzyme by using HM-30181A, a potentially specific inhibitor of the efflux transporter.

Other complication during intestinal drug absorption would be the possibility of the chemical loss of the active ingredient in the gastrointestinal lumen by the decomposition. In general, active ingredient is dissolved from the dosage from depending on its physicochemical/pharmaceutical properties. Since the rate/extent of absorption is a function of the amount/concentration of the drug in the intestine, the instability in the intestine would be one of the key factors in determining the oral bioavailability. The intestinal stability may be dependent on various reactions in the intestine, enzymatic or non-

enzymatic. For example, acid hydrolysis of penicillin G may occur in the stomach thereby leading to a loss of activity (György et al., 1945). Enzymatic reaction caused by digestive enzymes (e.g., in the pancreatic fluid), metabolic enzyme and enzymes from microflora may affect the stability of drugs in the intestine. For example, intestinal esterases hydrolyzed ester-type drugs such as aspirin, clofibrate, indanyl carbenicillin and procaine (Inoue et al., 1980). In addition, the absorption of glycerol and glycerides may undergo a complicated enzymatic reactions, as evidenced by their rapid decomposition during the digestion / absorption processes (Senior, 1964; Humberstone and Charman, 1997). Therefore, the limitation of bioavailability of a monoacetyldiglyeride, EC-18, by its intestinal instability, potential caused by intestinal esterase(s), was studied in part II of the thesis.

PART I

Enhanced intestinal absorption of indinavir and its metabolic conversion to M6 by the co-administration of HM-30181A, a P-glycoprotein inhibitor

1. Introduction

It is now well established that the intestinal P-glycoprotein (P-gp), an efflux transporter, limits the absorption of variety of drugs (Wacher et al., 1998; Lee et al., 2005; Murakami and Takano, 2008). For example, the AUC of orally administered imatinib, a P-gp substrate, was increased approximately 3 to 4-fold when elacridar and pantoprazole, both P-gp substrates were co-administered (Oostendorp et al., 2009). In addition, some food substances such as grapefruit juice may strongly inhibit the action of the efflux transporter thereby leading to a significant increase in the absorptive transport of P-gp substrates (e.g., talinolol) in Caco-2 monolayers (e.g., talinolol) (Spahn-Langguth and Langguth, 2001).

While it was originally thought that compounds with hydrophobic amine were primarily subjected to the efflux transport by P-gp (Bönisch et al., 1978), it is now increasingly evident that the substrate specificity is much wider for the transporter so that certain neutral / acidic compounds may also be the substrate (Putnam et al., 2002) to the transporter. Interestingly, CYP metabolizing enzymes, particularly CYP3A, also possess wide substrate specificity and, as a result, a significant portion of P-gp substrates may also be the substrate to the metabolizing enzymes as well. Theoretically, P-gp may render the dual substrates to 'recycling' during their absorption thereby leading to the prolongation of mean absorption time and to the enhancement

in intestinal metabolism. However, the experimental observation on the pharmacokinetic impact for the shared specificity appeared to be quite controversial. For example, it was proposed that, for a drug subjected to both P-gp mediated transport and CYP3A metabolism, the action of the efflux transporter may render the enhanced intestinal first pass metabolism of the drug by prolonging the mean absorption time (Johnson et al., 2001; Cummins et al., 2002; Cummins et al., 2003). On the contrary, however, others found that P-gp decreased metabolism of the dual substrate in the intestine in in/ex vivo study or theoretical analysis (Lan et al., 2000; Tam et al., 2003). Furthermore, other examples indicate that P-gp had little or no significant effect on intestinal first pass metabolism (Kato et al., 2003; Dufek et al., 2013). Currently, the underlying reason(s) for the complicated outcome is (are) not known. In the literature, however, the experimental design, particularly the use of P-gp / CYP3A inhibitor, was not consistent amongst the studies so that the results may not be directly compared. Furthermore, even for the studies using P-gp deficient mice to address the interplay between P-gp and CYP, the possibility of compensatory mechanism was not adequately examined (van Waterschoot and Schinkel, 2011).

Some of the discrepancies in the study of the 'recycling' on the intestinal first pass effect of drugs that are substrates for both the metabolizing enzymes and the efflux transport are likely to be originated from the lack of specific inhibitor of P-gp. HM-30181A, 4-oxo-4H-chromene-2-carboxylic

acid, [2-(2-{4-[2-(6,7-dimethoxy-3,4-dihydro-1H-isoqui-nolin-2-yl)-ethyl]-phenyl}-2H-tetrazol-5-yl)-4,5-dimethoxyphenyl]amide, was recently developed as a P-gp inhibitor to enhance the oral bioavailability of paclitaxel (Paek et al., 2006b). The new P-gp inhibitor was relatively potent and apparently selective in comparison to other P-gp inhibitors such as cyclosporine A, XR9576 and GF120918 (Kwak et al., 2010). Unfortunately, however, the possibility of the inhibitor for CYP mediated metabolism was not previously examined. Furthermore, the impact of the compound on the function of SLC transporters is not known. The objectives of this study, therefore, were two-fold: to determine the effect of HM-30181A on the activities of major CYP isozymes / SLC transporters, and to study the contribution of P-gp recycling in the intestinal first pass metabolism of a model substrate for P-gp and CYP3A using HM-30181A. In this study, indinavir was selected as a model substrate since the antiviral agent is known to have an extremely high efflux ratio (e.g., 15 in Caco-2 cell monolayer) due to the action of P-gp (Rouquayrol et al., 2002) while it is primarily metabolized by CYP3A (Lin et al., 1996). The formation of M6, an N-depyridomethylated metabolite of indinavir [viz, 33 ~ 58% of the total metabolites (Lin et al., 1996), was also monitored as an index of the first pass effect in this study.

2. Materials and Methods

2.1 Chemicals and reagents

Indinavir, citric acid, formic acid, potassium phosphate monobasic, Hanks' balanced salts (HBSS), sodium bicarbonate, D-(+)-glucose, HEPES, glipizide [an internal standard (IS) in indinavir assay], phenacetin, diclofenac sodium salt, omeprazole, dextromethorphan, ketoconazole, (±)-metoprolol (+)-tartrate salt and N,N-dimethylacetamide (DMAc) were purchased from Sigma-Aldrich (St. Louis, MO). The metabolite of indinavir (M6; N-[2(R)-hydroxy-l(S)-indanyl]-5-[2(S)-(1,1-dimetyl-ethylaminocarbonyl)piperizin-1-yl]-4(S)-hydroxy-2(R)-phenylmethyl pentanamide) was synthesized in-house from indinavir. HM-30181A was generously provided by Hanmi Pharm. Co., Ltd. (Seoul, Korea). Testosterone was purchased from Tokyo Chemical Industry Co. (Tokyo, Japan). [^{3}H] Digoxin (29.8 Ci/mmol) and [^{14}C] mannitol (57.1 mCi/mmol) were obtained from PerkinElmer (Waltham, MA). Dulbecco's modified Eagle's medium (DMEM), non-essential amino acid solution (NEAA), Dulbecco's phosphate buffered saline (DPBS), penicillin-streptomycin and fatal bovine serum (FBS) were also obtained from WelGENE (Gyeongsangbuk-do, Korea). Polyethylene glycol 400 (PEG 400) [Duksan Pure Chemicals (Gyeonggi-do, Korea)] was also used in this study. Caco-2 cells were obtained from American Type Culture Collection (Rockville, MD). MDCKII cells were provided by Dr. Borst in the Netherland Cancer Institute (Amsterdam, Netherland). Collagen-coated Transwell®

inserts (0.4 μm membrane pore size, 1.12 cm^2 surface area; product no. 3493) were purchased from Corning Inc. (Kennebunk, ME). Pooled male rat liver microsomes and nicotinamide adenine dinucleotide phosphate oxidase (NADPH) regenerating system solutions were purchased from Corning Gentest (Woburn, MA). Zoletil (Tiletamine-HCl/zolazepam-HCl) was obtained from Virbac Laboratories (Carros, France) or Rompun (xylazine-HCl) from Bayer Corp. (Shawnee Mission, KS). Solvents were of HPLC grade and obtained from Fisher Scientific (Pittsburgh, PA). All chemicals were used without further purification.

2.2 Animals

Male Sprague-Dawley (SD) rats, weighing 250 to 350 g, were used in this study (Orient Bio Inc., Gyeonggi-do, Korea) and maintained on a 12 h light/dark cycle with free access to food and water at the Seoul National University Institutional Animal Care Facility and acclimatized for at least 3 days before studies. Animals used in all studies were fasted 24 h. When it was necessary to anesthetized rats, the animals received tiletamine/zolazepam (20 mg/mL) and xylazine (4 mg/mL) solution at a dose of 1 mL/kg by intramuscular administration. All studies were reviewed and approved by the Seoul National University Institutional Animal Care and Use Committee according to the National Institutes of Health Publication Number 85-23 Principles of Laboratory Animal Care revised in 1985.

2.3 In vitro Studies

2.3.1. Potential Inhibition of CYP-mediated Metabolisms by HM-30181A in Rat Liver Microsomal Incubations

The potential of HM-30181A for inhibiting major rat CYP enzymes (1A2, 2C9, 2C19, 2D6 and 3A4) was studied in a system consisting of rat liver microsomes (RLMs) and NADPH regenerating system. The reaction mixture (final volume of 1 mL) consisted of 0.5 mg/mL RLMs, 10 μM HM-30181A in a vehicle (DMAc:PEG400:saline = 1:2:1), 0.1 M potassium phosphate (pH 7.4), 1.3 mM NADP+, 3.3 mM glucose-6-phosphate, 0.4 U/mL glucose-6-phosphate dehydrogenase and 3.3 mM $MgCl_2$. After equilibrated at 37˚C for 10 min, reaction was initiated by adding substrate [i.e., 10 μM phenacetin (1A2), 5 μM diclofenac (2C9), 1 μM omeprazole (2C19), 1 μM dextromethorphan (2D6), or 30 μM testosterone (3A4)] for major CYPs. The final concentration of each substrate was lower than reported K_m in RLMs (Kuntzman et al., 1965; Kerry et al., 1993; Bogaards et al., 2000; Easterbrook et al., 2001; Lee et al., 2007). The mixture was incubated in water bath at 37˚C and samples (100 μL) were collected at 0, 5 and 10 min (for the study of the involvement of CYP3A4) or 0, 5, 10 and 15 min (2C9, 2C19 and 2D6) or 0, 20, 40 and 60 min (1A2). The sample was then added with 100 μL of ice-cold acetonitrile to terminate the reaction. After vortexing for 10 min, samples were centrifuged at 16,100 g in 4˚C for 5 min. The concentration of the substrates in the supernatant from samples was measured using UV/LC

system (see below).

2.3.2. Potential Inhibition of SLC Transporters by HM-30181A in MDCKII/FRT cells Expressing the Transporters

To determine the interaction of HM-30181A with typical SLC transporters [organic anion transporting polypeptide 1b2 (rOatp1b2, orthologous form for hOATP1B1 and hOATP1B3 in human), organic anion transporter 1, 3 (rOat1, rOat3) and organic cation transporter 2 (rOct2)] were cloned and functionally expressed in MDCKII/FRT cells containing Flip-In system (Invitrogen, Carlsbad, CA) (Lee et al., 2015). Transfected MDCKII/FRT cells were seeded onto 24-well plates at a density of 500,000 cells/mL and were grown in Dulbecco's modified Eagle medium (DMEM, with 1 g/L of D-glucose) with 10% (v/v) fetal bovine serum (FBS), 1% (v/v) non-essential amino acid (NEAA), 100 units/mL penicillin/streptomycin and 10 mM HEPES. Seeded cells were placed in a humidified incubator at 37℃ and 5% CO2. After two days, the cells were washed three times and pre-incubated with transport media (TM, adjusted to pH 7.4 with sodium hydroxide). In this study, TM was consisted of 9.7 g/L HBSS, 2.38g/L HEPES and 0.35 g/L sodium bicarbonate. After 10 min, the medium was removed and replaced with the media containing the substrate [i.e., [^{3}H] estrone-3-sulfate (E3S; total concentration of 1 μM containing 3% labelled compound; substrates for rOatp1b2 and rOat3), [^{3}H] p-aminohippuric acid (PAH; total concentration of 2 μM containing 10% labelled compound; substrate for rOat1)

and [^{3}H] 1-methyl-4phenylpyridium (MPP+; total concentration of 1 μM containing 0.5% labelled compound; substrate for rOct2)] with or without corresponding inhibitor [i.e., atorvastatin (50 μM, rOatp1b2), probenecid (500 μM, rOat1 and rOat3), or diphenhydramine (300 μM, rOct2)]. When it was necessary, HM-30181A (100 μM) replaced the standard inhibitors for the transporters to study the potential inhibition of the transporters. In this study, the cells were incubated for 5 min to study the cellular accumulation (i.e, the uptake) of the substrate. Upon completion of the incubation, the medium was aspirated and cells washed three times with ice-cold Dulcecco's phosphate buffered saline (DPBS). After solubilization of cells with 0.2 N NaOH, the lysate was added with Ultima Gold (PerkinElmer, Waltham, MA) and the amount of substrate in the sample determined by liquid scintillation counter (Tri-Carb 3110 TR, PerkinElmer Life Science, Boston, MA). The uptake rate were normalized by protein concentration as determined by bicinchoninic acid (BCA) assay.

2.3.3. Transport of M6 in Caco-2 Cell Monolayers

When it was necessary to study whether M6, the major metabolite of indinavir in rats, is subjected to P-gp mediated transport, bi-directional transport of M6 were studied with or without verapamil (i.e., standard P-gp inhibitor) or HM-30181A in Caco-2 cells. In this study, the transport of [^{3}H] digoxin (standard P-gp substrate), [^{14}C] mannitol (low permeability marker)

or (±)-metoprolol (+)-tartrate salt (high permeability marker) were used as a standard compound in the cell monolayer. Caco-2 cells with passage number 43 were seeded onto 12-well collagen coated Transwell® at the density of 500,000 cells/mL and were grown in DMEM (with 4.5 g/L D-glucose) with 20% (v/v) FBS, 1% (v/v) NEAA, 1% (v/v) penicillin-streptomycin. Cells were, then, placed in a humidified incubator at 37℃ and 5% CO2 and the culture medium was replaced every two days. After 7 days, FBS concentration was changed to 10% (v/v). All bi-directional transport studies were conducted 21 days after seeding. Trans-epithelial electric resistance (TEER) was measured by Epithelial Voltohmmeter (EVOM, World Precision Instruments, Sarasota, FL) after washing cells three times with TM [9.7 g/L HBSS, 0.35 g/L sodium bicarbonate, 2.38 g/L HEPES, 1.95 g/L glucose, pH 7.35]. In this study, TEER value between 252 and 382 $\Omega \cdot cm^2$ was used (Press, 2011).

When it was necessary to study the transport of compounds from the apical side to basolateral side, donor solution (0.5 mL) containing [^{3}H] digoxin (1 μM), [^{14}C] mannitol (100 μM), metoprolol (50 μM) or M6 (10 μM) in the presence or the absence of the inhibitor (i.e., HM-30181A or verapamil) was added to the apical side while 1.5 mL of receiver solution [TM with or without inhibitor (verapamil or HM-30181A)] was added to the basolateral side. Samples (500 μL) were collected from the basolateral side and the fresh solution replaced to the basolateral compartment. To study the transport of compounds from the basolateral side to apical side, donor solution (1.5 mL)

was added to the basolateral side while 0.5 mL of the receiver solution was added to the apical side. In this study, samples (300 μL) were collected from the apical side and the fresh solution replaced to the apical compartment. All samplings were carried out at every 30 min intervals for 2 h while maintaining the temperature of 37℃ and the atmosphere of 5% CO_2. Aliquots of the sample (100 μL) were vortex-mixed with 200 μL of acetonitrile for 10 min, and the mixture centrifuged at 16,100 g at 4℃ for 5 min. The supernatant was transferred and stored at -20℃ until the analysis by LC-MS/MS (for M6) or liquid scintillation counting (low / high permeability marker).

2.4 Intestinal Transport and Metabolism of Indinavir in Ex Vivo

To determine the transport and metabolism of indinavir in the intestine in ex vivo conditions, Ussing chamber study was carried out, similar to the method described previously (Boisset et al., 2000; Li et al., 2002; Haslam et al., 2011). Briefly, a 10 cm segment of the ileum was carefully dissected from anesthetized rats and the excised tissue was immediately added to freshly prepared TM (4˚C) with O_2/CO_2 (95:5) bubbling. The ileum segment was cut into four to five 2 cm pieces to avoid Peyer's patches and the cylindrical segments were cut along the mesenteric border line to expose the luminal side. The rectangular tissue piece was then mounted on the half of a

diffusion chamber with six fixing pins: The serous membrane was then removed immediately after the fixation. After the assembly of two halves of the chamber, 2 mL of TM (with or without 100 μM HM-30181A) was added to each compartment and the device pre-incubated for 20 min with carbogen bubbling at 37℃.

In this study, the tissue having the TEER of at least 95 $\Omega \cdot cm^2$ (viz, the resistance measured just prior to the mounting) was used. After the equilibration for 20 min, the medium was removed and replaced with 2 mL of pre-warmed TM to the receiver side / 2 mL of pre-warmed TM containing 5 μM indinavir to the donor side. When it was necessary to study the effect of HM-30181A, the inhibitor at 100 μM was added to both sides. The tissue was incubated with carbogen bubbling at 37℃ and samples (100 μL) were collected every 30 min intervals from both sides of chamber up to 2 h. Upon completion of the incubation, the mounted tissue was washed ten times with 1 mL of ice-cold TM. The tissue was, then, collected and homogenized for 1 min with a sonic dismembrator in 4-fold weight of TM and ice-cold 2 N NaOH solution (50:50, v/v). The homogenate was added with acetonitrile (1:3, v/v, 200 mL of total volume) containing glipizide (100 ng/mL) and the mixture vortexed-mixed for 10 min. The mixture was centrifuged at 16,100 g at 4℃ for 5 min, and the supernatant was collected / stored at -20℃ until the analysis for indinavir and M6.

2.5 In vivo Studies

For intravenous administration study, previously reported method was used (Ahn et al., 2004; Koo et al., 2005). Briefly, rats (250~300 g) were anesthetized with tiletamine/zolazepam (20 mg/mL) and xylazine (4 mg/mL) solution at a dose of 1 mL/kg by intramuscular administration to catheterize a polyethylene tubing (PE-50; Clay Adams, Parsippany, NJ) in the right femoral artery for blood sampling and vein for drug administration under the light anesthetization. Control rats (N = 5) received only the vehicle (DMAc:PEG400:saline = 1:2:1, v/v/v; administration volume at 2 ml/kg) orally in addition to a single intravenous dose of indinavir at 1 or 10 mg/kg. In this control study, the vehicle was administered 10 min before the injection. The drug was injected (injection volume at 1 mL/kg) as a solution in 0.05 M citric acid. At pre-determined time points (0, 2, 5, 15, 30, 60, 90 and 120 min), blood samples (150 μL each) were collected. For HM-30181a group, rats (N = 4) received a single oral dose of HM-30181A at 10 mg/kg while maintaining other experimental conditions.

For oral administration study, surgical procedures and other administration conditions, including indinavir dosing vehicle, were identical to the intravenous administration study except that indinavir was given orally. In this study, blood samples were collected at 0, 5, 15, 20, 25, 30, 45, 60, 90 and 120 min after the oral administration of indinavir.

For intra-portal vein infusion study, rats were catheterized in the right femoral artery, vein and portal vein for blood sampling and drug administration. Indinavir solution was infused to rats through the poral vein cannulae at the rate of 62.5 μg/min for 20 min. Ten min prior to the initiation of the infusion, rats orally received HM-30181A (10 mg/kg) or the vehicle. Blood samples were collected at 0, 5, 15, 20, 25, 30, 45, 60, 90 and 120 min after the initiation of the infusion.

Collected blood samples were immediately centrifuged at 16,100 g for 10 min at 4℃, and the supernatants were collected / stored at -20℃ until the analysis for indinavir / M6 by LC-MS/MS (see below).

2.6 Kinetic model for ex vivo results on intestinal metabolism to M6 and transport of indinavir

In this study, a relatively specific P-gp inhibitor (e.g., HM-30181A) was used to affect the efflux process of indinavir in ex vivo studies involving Ussing chambers. To ascertain whether the results from the ex vivo study were kinetically consistent with the cooperative effect of P-gp and intestinal metabolism, a simulation study was carried out for the formation of M6 in the presence and the absence of P-gp inhibition. In this study, the kinetics of P-gp efflux or metabolism was assumed to follow a simple Michaelis-Menten kinetics using relevant pharmacokinetic parameters from the literatures (Table

1) (Hochman et al., 2000). In particular, a three compartment model (Fig. 1) was taken into consideration for the kinetics of indinavir across and in the intestinal tissue. Therefore, the differential equations for the model presented as follows:

$$V_D \frac{dI_D}{dt} = -PS_1 \cdot I_D + (PS_1 + CL_{eff}) \cdot I_C \quad (1)$$

$$V_C \frac{dI_C}{dt} = PS_1 \cdot I_D + PS_2 \cdot I_R - (PS_1 + CL_{eff} + PS_2 + CL_m) \cdot I_C \quad (2)$$

$$V_R \frac{dI_R}{dt} = PS_2 \cdot (I_C - I_R) \quad (3)$$

$$V_D \frac{dM_D}{dt} = -PS_{1'} \cdot M_D + (PS_{1'} + CL_{eff'}) \cdot M_C \quad (4)$$

$$V_C \frac{dM_C}{dt} = PS_{1'} \cdot M_D + CL_m \cdot I_C + PS_{2'} \cdot M_R - (PS_{1'} + CL_{eff'} + PS_{2'}) \cdot M_C \quad (5)$$

$$V_R \frac{dM_R}{dt} = PS_{2'} \cdot (M_C - M_R) \quad (6)$$

Where I_D, I_C, and I_R are the concentration of indinavir in donor, intracellular, and receiver compartments, respectively; M_D, M_C, and M_R are the concentration of M6 in donor, intracellular, and receiver compartments, respectively; V_D, V_C, and V_R are the volume of donor, intracellular, and receiver compartments, respectively; PS_1 and PS_2 are the passive permeability-surface area product of indinavir between donor and intracellular compartment, and between intracellular and receiver compartment, respectively; $PS_{1'}$ and $PS_{2'}$ are the passive permeability-surface area product

of M6 between donor and intracellular compartment, and between intracellular and receiver compartment, respectively; CL_{eff} and $CL_{eff'}$ are the efflux clearance mediated by P-gp of indinavir and M6 respectively; CL_m is the formation clearance of M6 from intracellular indinavir. In this study, the receiver compartment was assumed to be under a sink condition so that the drug / metabolite movement from the acceptor to the tissue is practically negligible. For the purpose of simulation, PS_1 and PS_2 were assumed to be identical to each other, and estimated from the apparent permeability (P_{app}) obtained from the ex vivo study.

2.7 Analytical Procedure

2.7.1. High performance liquid chromatography for RLM studies

The concentration of standard CYP substrates in RLM incubations was determined by HPLC-UV system (Waters e2695 HPLC, Waters 2489 UV system). Samples (100 μL) were added with 100 μL ice-cold acetonitrile and vortexed for 10 min. After the centrifugation at 16,100 g at 4℃ for 10 min, the supernatant was collected / transfered and 100 μL of the aliquot was directly injected onto a Gemini-NX 5 μ C18 (150 X 4.6 mm) column. In this study, the flow rate at 1 mL/min was used. For analysis of phenacetin (1A2), diclofenac (2C9), omeprazole (2C19) and dextromethorphan (2D6), the

mobile phase consisted of (A) acetonitrile and (B) phosphate buffer (20 mM). Linear gradient was utilized for the analysis of the substrate as mobile phase of (A):(B) was 20:80 to 56:44 in 6 min for phenacetin, 55: 45 to 82:18 in 6 min for diclofenac, 30:70 to 45:55 in 3.5 min for omeprazole or 20:80 to 47:53 in 6 min for dextromethorphan, respectively. For analysis of testosterone, the isocratic method was used. Mobile phase (A) and (B) were the mixture of acetonitrile and water in 5:95 and 80:20, respectively, and adjusted to pH with trifluoroacetic acid at 3.4. In this study, the flow of mobile phase (A):(B) was 50:50. The absorbance at 245, 254, 302, 280 or 254 nM was monitored for the determination of phenacetin, diclofenac, omeprazole, dextromethorphan or testosterone, respectively.

2.7.2. Liquid chromatography-Tandem mass spectrometry assay for indinavir and M6

For the determination of indinavir / M6 concentrations in ex vivo and in vitro studies, the sample (100 μL) form Caco-2 cells study or Ussing chamber study was added with 200 μL acetonitrile. For the determination of the concentration of the drug / metabolite, in vivo samples (50 μL) were added with 200 μL acetonitrile containing glipizide (100 ng/mL; an internal standard) for deproteination. The mixture was then vortexed for 10 minutes and centrifuged at 16,100 g at 4℃ for 5 min. An aliquot (100 μL) of the supernatant was collected / transfered / injected (5 μL) onto LC-MS/MS. The LC-MS/MS system comprised Waters e2695 HPLC (Milford, MA) and API

3200 QTrap (Applied Biosystems, Foster City, CA). The mobile phases consisted of (A) 0.1% formic acid in acetonitrile and (B) 0.1% formic acid in water. The flow was performed at a flow rate of 0.3 mL/min with a gradient of 60% mobile phase (A) for 0.5 min, 60% to 75% mobile phase (A) for 0.1 min, 75% mobile phase (A) for 0.4 min, 75% to 60% mobile phase (A) for 0.1 min, 60% mobile phase (A) for 3.9 min and 5 µL of sample was injected onto an Eclipse XDB-C18, 3.5 µm, 2.1 X 100 mm (Agilent Technologies, Santa Clara, CA). The samples were ionized using turbo ion spray interface in the positive ionization mode and monitored at the following Q1/Q3 transitions (m/z): 614.1/421.1 for indinavir, 523.3/273.2 for M6 and 445.8/320.9 for glipizide. The common source/gas of indinavir and M6 was followed. The ion spray voltage, source temperature and pressure of the curtain gas were 5500 V, 500°C and 10 psi. The declustering potentials (DP) for indinavir, M6 and glipizide were 51, 56 and 47.5 V, respectively. The entrance potentials (EP) were 5.2, 5.5 and 4.02 V, collision energies (CE) were 42, 41 and 17 V and the collision cell exit potentials (CXP) were 6.0, 4.0 and 8.0 V, respectively. Calibration curves for indinavir ranged from 10 to 5000 nM for in vitro / ex vivo study and from 10 to 10000 ng/mL for in vivo studies, and were linear (r^2 > 0.998) for all experimental conditions. In this study, the accuracy ranged from 88 to 108% for the indinavir assay. For the calibration curve for M6 ranged from 5 to 10000 nM for in vitro studies, from 5 to 250 nM for ex vivo study and from 5 to 500 ng/mL for in vivo studies. All calibration curves for

M6 were found linear ($r^2 > 0.998$), with the accuracy ranged from 88 to 113%.

2.8 Data Analysis

For RLMs inhibition studies, microsomal intrinsic clearance (CL_{int}) of each enzyme substrate was calculated by eq. 5

$$CL_{int} = \frac{K_{el}}{[microsome]} \times \frac{mg\ microsomal\ protein}{g\ liver} \times \frac{g\ liver}{kg\ body\ weight} \qquad (7)$$

where K_{el} represents the elimination rate constant ($minute^{-1}$) and [*microsome*] represents the protein concentration in the microsomal incubation (mg/mL). The parameters of *mg microsomal protein/g liver* and *g liver/kg body weight* was obtained from the literature (Houston, 1994; Bayliss, 1999; Naritomi et al., 2001).

When it was necessary to determine M6 permeability, the apparent permeability (P_{app}) of M6 in Caco-2 cell monolayers and indinavir across the rat intestinal tissue in ex vivo studies were calculated according to eq. 6 (Mouly et al., 2004).

$$P_{app} = \frac{dQ}{dt} \times \frac{1}{S \cdot C_0} \qquad (8)$$

where P_{app} is apparent permeability coefficient (cm/sec), *dQ/dt* is the flux (μg/sec), *S* is the surface area of the culture insert (cm^2) or tissue (cm^2) and C_0 is the initial concentration of M6 in the donor side.

For the calculation of the efflux ratio of M6 in Caco-2 cell

monolayers, the ep. 7 was used.

$$\mathrm{ER} = \frac{P_{app,B\ to\ A}}{P_{app,A\ to\ B}} \tag{9}$$

where *ER* represents the efflux ratio, $P_{app,\ B\ to\ A}$ apparent permeability from basolateral side to apical side, and $P_{app,\ A\ to\ B}$ apparent permeability from apical side to basolateral side.

For the kinetic analysis of the plasma concentration versus time data for indinavir and M6, standard moment analysis was carried out by using the WinNonlin software (Ver. 3.1; Pharsight, Mountain View, CA, USA) running on a PC. The area under the indinavir and M6 concentration in the plasma-time curve from time zero to infinity (AUC_{inf}) and the area under the respective first moment–time curve from time zero to infinity ($AUMC_{inf}$) were calculated by the linear trapezoidal method and the standard area extrapolation method (Gibaldi et al., 1982). The mean residence time (MRT) was calculated $AUMC_{inf}$ divided by AUC_{inf}. In this study, systemic clearance (CL), half-life ($T_{1/2}$) and steady-state volume of distribution (V_{ss}) were also calculated assuming the first order kinetics for indinavir and M6. When necessary, the maximum indinavir concentration (C_{max}) and the time point at C_{max} (T_{max}) were read directly from the time-concentration profile in the plasma.

3. Results

3.1 Interaction of HM-30181A with CYP-mediated Metabolism in RLMs and with Uptake Transporters in Transporter-expressing MDCKII/FRT Cells

The amount remaining (in percent of the initial amount) for each substrate [i.e., phenacetin (1A2), diclofenac (2C9), omeprazole (2C19), dextromethorphan (2D6) and testosterone (3A4)] was about 80, 90, 25, 29 and 13% of at the last sampling time [i.e., 0, 20, 40 and 60 min (1A2); 0, 5, 10 and 15 min (2C9, 2C19 and 2D6); 0, 5 and 10 min (3A4)]. There was no statistical difference in amount remaining at the last sampling time between the control and HM-30181A group (Fig. 2). As a result, there was no statistical difference in intrinsic clearances in microsomes for each substrate between the two groups (Table 2). The uptake of the substrate (E3S for rOatp1b2 and rOat3, PAH for rOat1 or MPP+ for rOct2) in the corresponding transporter-expressing MDCKII/FRT cells was 23.0 ~ 91.4% deceased by the presence of their representative inhibitors (atorvastatin, probenecid and diphenhydramine) when compared with that of the control (i.e., no inhibitor). In contrast, the presence of HM-30181A did not affect the cellular uptake of the substrates in transporter-expressing MDCKII/FRT cells (Fig. 3). These results suggest that HM-30181A has no inhibitory effect on CYP-mediated metabolism and on SLC transporter-mediated transport.

3.2 Bi-directional Transport Study of M6 in Caco-2 Cell Monolayers

In this study, bi-directional transport study of M6 was examined with or without HM-30181A or verapamil in Caco-2 cell monolayers. In this experimental system, the apparent permeability for [^{14}C] mannitol (i.e., a low permeability marker), metoprolol (i.e., a high permeability marker) and [^{3}H] digoxin (i.e., a standard P-gp substrate) 2.26 ± 0.14, 26.3 ± 1.1 and 4.42 ± 0.33 x 10^{-6} cm/sec for transport from the apical side to basolateral side in Caco-2 cells, respectively. The transport permeability in the reverse direction (from the basal side to the apical side) was 2.40 ± 0.10, 30.5 ± 1.2 and 18.9 ± 1.0 x 10^{-6} cm/sec for the three reference compounds, respectively. As a result, estimated efflux ratio was 1.06, 1.16 and 4.28 for mannitol, metoprolol and digoxin, respectively. Under this experimental condition, the apparent permeability of the transport of M6 from the apical to basal side of Caco-2 cells was 36.5% increased by HM-30181A while there was no change in the transport by verapamil. For the case of the transport in the reverse direction (i.e., from the apical to basolateral side), the M6 transport was 54.3 and 66.3% decreased by HM-30181A and verapamil treatment, compared with that without the inhibitor (Fig. 4). The efflux ratio of M6 was 3.23 without the inhibitor and the value decreased to 1.08 by HM-30181A treatment and to 1.03 by verapamil treatment. These observations suggest that M6 has low permeability, probably by the action of efflux transporter(s) such as P-gp.

3.3 Inhibitory Effect of P-gp Inhibition by HM-30181A on Absorption and Metabolism of Indinavir in Rats

When pretreated with HM-30181A, the systemic exposure of indinavir was approximately 34% increased after intravenous injection dose of 1 mg/kg (Fig. 6A; Table 4). However, the M6 was below the quantification limit of the assay, so that the pharmacokinetics analysis could not be attempted. When the intravenous dose of indinavir was adjusted to 10 mg/kg, the systemic exposure of indinavir, as well as the formation of M6, was not affected (i.e., $AUC_{M6}/AUC_{indinavir}$ was 4.60 ± 0.41 and 4.72 ± 1.88% in the absence and presence of HM-30181A) by the administration of the inhibitor (Fig. 6B; Table 4). For the case of the oral administration of indinavir, the systemic exposure was approximately 2-fold increased ($p < 0.05$) for both indinavir and M6: C_{max} of indinavir was similarly increased ($p < 0.05$, about 2.5-fold) by HM-30181A co-administration (Fig. 6C; Table 4). As a result, the $AUC_{M6}/AUC_{indinavir}$ was not statistically different (i.e., 10.5 ± 1.4 and 9.95 ± 1.8% for the control and HM-30181A treatment) between the two groups. However, the AUC ratio of the oral administration study was approximately twice the AUC ratio from the high dose intravenous injection study. These results suggest that inhibition of intestinal and hepatic P-gp by HM-30181A leads to a similar increase in the absorption of indinavir and formation of M6. When indinavir was infused to portal vein infusion for 20 min, the profile of the plasma concentration of indinavir in the systemic circulation showed clear

distinction 45 min of the indinavir infusion (Fig. 6D) by the administration of HM-30181A. The AUC of indinavir and M6 was approximately 2.5- and 1.9-fold increased ($p < 0.05$) by HM-30181A, respectively, whereas C_{max} of indinavir and M6 was not apparently affected by the inhibitor (Table 4). Accordingly, the $AUC_{M6}/AUC_{indinavir}$ was statistically different ($p < 0.05$) between the two groups (i.e., 6.12 ± 0.32 and 4.79 ± 0.52% for control and HM-30181A groups), indicating hepatic elimination (e.g., biliary excretion) of indinavir/M6 was affected by HM-30181A.

3.4 Transport of Indinavir and Formation of M6 in Ussing Chambers

When the intestinal tissue was pre-treated with HM-30181A, the apparent permeability of indinavir was 52.3% increased compared with the control (Table 5). Under this experimental condition, the M6 concentration in the receiver and donor side was below the quantification limit of assay. The accumulation of indinavir in intestinal tissue tended to increase by the inhibitor pre-treatment although statistical different was not noted in the experiment (Table 5). In contrast, the amount of M6 in the intestine was 40.8% increased by the pretreatment (Table 5). The increased amount of M6 in the intestinal tissue was consistent with a kinetic model assuming an interplay between P-gp mediated recycling and intestinal metabolism of indinavir (Fig. 5). These observations indicate that the inhibition of intestinal P-gp by HM-

30181 leads to an increase in the apparent permeability of indinavir and the formation of M6 in the tissue.

4. Discussion

Indinavir, a protease inhibitor for anti-retroviral therapy, was originally developed in 1990's (Dorsey et al., 1994; Lin et al., 1995; Lin, 1999) and is a well known substrate for both P-gp and CYP3A4. In particular, the anti-viral drug is almost metabolized by one major metabolic enzyme, CYP3A4, during its elimination process (Chiba et al., 1996; Lin et al., 1996; Chiba et al., 1997). The drug is also reported to possess a high efflux ratio, rendered by the action of P-gp (Kim et al., 1998; Rouquayrol et al., 2002; Balimane et al., 2004; Varma et al., 2005). Therefore, this drug would undergo a significant recycling during its intestinal absorption. Indeed, indinavir has been regarded as an attractive model drug for the study of the interplay between the recycling and intestinal first pass effect (Lin et al., 1999b). HM-30181A, the P-gp inhibitor used in this study, does not appear to affect CYP-mediated metabolism (Fig. 2) nor the activities of SLC transporters (Fig. 3), suggesting that the inhibitor is selective for P-gp (Paek et al., 2006a; Paek et al., 2006b; Paek et al., 2007; Kwak et al., 2010) and is useful in the study of the interplay between P-gp mediated efflux and intestinal metabolism.

To study the effect of the efflux on the intestinal first pass metabolism, the pharmacokinetics of indinavir and M6, the major metabolite, was studied in the presence and the absence of HM-30181A in rats. It was found that the pretreatment with the inhibitor led to comparable increase in the AUC for the drug and the metabolite: The 'metabolic ratio' (i.e., the AUC ratio) was

apparently not affected by the inhibitor treatment (Table 4) in this in vivo study. Therefore, this observation could be potential indication for the absence of the interplay effect. However, to confirm the lack of the effect, the possibility of 'masking' has to be ruled out. That is, unchanged exposure of dual substrates for P-gp and the metabolizing enzyme by P-gp inhibitor treatment or in P-gp gene knock out mice has been previously attributed to the 'masking effect' rendered by the saturation of the hepatic P-gp. Therefore, additional in vivo studies with the intravenous administration of indinavir were found necessary.

The plasma concentrations of indinavir were slightly increased by HM-30181A at the intravenous indinavir dose at 1 mg/kg. However, the M6 concentration was not detectable probably because of the indinavir dosage was not sufficient. When the indinavir dosage was increased, the AUCs for the drug and the metabolite were not affected by HM-30181A pretreatment at the intravenous indinavir dose at 10 mg/kg (Fig. 6B, Table 4), suggesting that the 'masking' effect may not be adequately ruled out in the higher dosage. Furthermore, it is also possible that the dosage of HM-30181A is not sufficient for the P-gp inhibition in the canalicular membrane. To examine this possibility, the concentration of HM-30181A in the blood and the liver was measured after the oral administration. We found that the inhibitor was not detected in the plasma while the liver concentration was readily measured [i.e., 38.1 ± 15.3 and 505 ± 124 nM at 30 and 130 min after the inhibitor

administration, respectively (Appendix A)]. Based on the literature reports, it was estimated that, after 30 min of the inhibitor administration, the hepatic P-gp would have been inhibited (Kwak et al., 2010).

To rule out the possibility of masking effect, portal vein infusion study was carried out. In this study, we were particularly interested in the range of indinavir concentration achieved by this administration condition so that the range obtained here would be comparable to that from the oral administration study. We found that a statistical difference was noted for the AUC of indinavir and M6 between the two groups (Fig. 6D, Table 4). In particular, the AUC was 2.5- and 1.9-fold higher ($p < 0.05$) for the drug and the metabolite, respectively, by HM-30181A treatment, suggesting that the net metabolite formation during the intestinal metabolism would be higher by the inhibitor treatment (Table 4). It was also found from in vitro experiment with Caco-2 cells that the efflux ratio for M6 was 3.23 and the value decreased to 1.08 by P-gp inhibition, suggesting that the metabolite is also subjected to P-gp mediated efflux. In previous studies, the efflux ratio for indinavir was 7 ~ 15 in Caco-2 cells (Rouquayrol et al., 2002; Balimane et al., 2004; Varma et al., 2005).

To further confirm the interplay effect on M6 formation by intestinal P-gp, ex vivo studies with Ussing chambers were carried out. As expected, the apparent permeability was increased for the indinavir transport across the intestinal tissue by the inhibitor treatment ($p < 0.05$) (Table 5). Interestingly,

the increased permeability was associated with no difference in indinavir amount in the tissue while the M6 amount in the tissue was slightly but distinctly increased ($p < 0.05$). For the case of M6 in the donor and the receiver, the concentration was not detectable. These results supported the result of oral administration study in that the action of the intestinal P-gp may render a decrease of the metabolism to M6 during the intestinal absorption of indinavir.

In summary, HM-30181A had no appreciable effect on major drug metabolizing enzymes nor on typical SLC transporters. In Caco-2 cell monolayer study, M6 has a low permeability (i.e., $0.586 \pm 0.039 \times 10^{-6}$ cm/sec), which could be due to a potential substrate to efflux transporter(s) (i.e., efflux ratio of 3.2) such as P-gp. Only a minor increase in the 'metabolic ratio' was noted after the simultaneous administration of indinavir and HM-30181A orally. Interestingly, however, intraportal vein administration of indinavir led to a decrease in the 'metabolic ratio' of M6 by oral HM-30181A. Taken together, a small increase in the formation of M6 in the intestine may have occurred by the presence of the P-gp inhibition. In Ussing chamber experiment, the amount of M6 in the intestine was found to be increased by the pretreatment of HM-30181A, in support of the enhanced effect found in vivo. Therefore, these observations collectively suggest that 'P-gp mediated recycling' decrease metabolic ratio, although not to a substantial extent, in rats.

5. References

Ahn SH, Jeon SH, Tsuruo T, Shim CK, and Chung SJ (2004) Pharmacokinetic characterization of dehydroevodiamine in the rat brain. *Journal of pharmaceutical sciences* **93:**283-292.

Bönisch H, Graefe K-H, and Trendelenburg U (1978) The determination of the rate constant for the efflux of an amine from efflux curves for amine and metabolite. *Naunyn-Schmiedeberg's archives of pharmacology* **304:**147-155.

Balimane PV, Patel K, Marino A, and Chong S (2004) Utility of 96 well Caco-2 cell system for increased throughput of P-gp screening in drug discovery. *European journal of pharmaceutics and biopharmaceutics* **58:**99-105.

Bayliss M (1999) Utility of hepatocytes to model species differences in the metabolism of loxtidine and to predict pharmacokinetic parameters in rat, dog and man. *Xenobiotica* **29:**253-268.

Benet LZ, Wu C-Y, Hebert MF, and Wacher VJ (1996) Intestinal drug metabolism and antitransport processes: A potential paradigm shift in oral drug delivery. *Journal of controlled release* **39:**139-143.

Bogaards J, Bertrand M, Jackson P, Oudshoorn M, Weaver R, Van Bladeren P, and Walther B (2000) Determining the best animal model for human cytochrome P450 activities: a comparison of mouse, rat, rabbit, dog, micropig, monkey and man. *Xenobiotica* **30:**1131-1152.

Boisset M, Botham RP, Haegele KD, Lenfant B, and Pachot JI (2000) Absorption of angiotensin II antagonists in Ussing chambers, Caco-2, perfused jejunum loop and in vivo:: Importance of drug ionisation in the in vitro prediction of in vivo absorption. *European Journal of Pharmaceutical Sciences* **10:**215-224.

Chiba M, Hensleigh M, and Lin JH (1997) Hepatic and intestinal metabolism of indinavir, an HIV protease inhibitor, in rat and human microsomes: major role of CYP3A. *Biochemical pharmacology* **53:**1187-1195.

Chiba M, Hensleigh M, Nishime JA, Balani SK, and Lin JH (1996) Role of cytochrome P450 3A4 in human metabolism of MK-639, a potent human immunodeficiency virus protease inhibitor. *Drug metabolism and disposition* **24:**307-314.

Cummins CL, Jacobsen W, and Benet LZ (2002) Unmasking the dynamic interplay between intestinal P-glycoprotein and CYP3A4. *Journal of Pharmacology and Experimental Therapeutics* **300:**1036-1045.

Cummins CL, Salphati L, Reid MJ, and Benet LZ (2003) In vivo modulation of intestinal CYP3A metabolism by P-glycoprotein: studies using the rat single-pass intestinal perfusion model. *Journal of Pharmacology and Experimental Therapeutics* **305:**306-314.

Dorsey BD, Levin RB, McDaniel SL, Vacca JP, Guare JP, Darke PL, Zugay JA, Emini EA, and Schleif WA (1994) L-735,524: the design of a potent and orally bioavailable HIV protease inhibitor. *Journal of medicinal chemistry* **37:**3443-3451.

Dufek MB, Knight BM, Bridges AS, and Thakker DR (2013) P-glycoprotein increases portal bioavailability of loperamide in mouse by reducing first-pass intestinal metabolism. *Drug Metabolism and Disposition* **41:**642-650.

Easterbrook J, Fackett D, and Li AP (2001) A comparison of aroclor 1254-induced and uninduced rat liver microsomes to human liver microsomes in phenytoin O-deethylation, coumarin 7-hydroxylation, tolbutamide 4-hydroxylation, S-mephenytoin 4′-hydroxylation, chloroxazone 6-hydroxylation and testosterone 6β-hydroxylation. *Chemico-biological interactions* **134:**243-249.

Elferink RPO, Meijer DK, Kuipers F, Jansen PL, Groen AK, and Groothuis GM (1995) Hepatobiliary secretion of organic compounds; molecular mechanisms of membrane transport. *Biochimica et Biophysica Acta (BBA)-Reviews on Biomembranes* **1241:**215-268.

György P, Vandegrift H, Elias W, Colio L, Barry F, and Pilcher J (1945) Administration of penicillin by mouth: preliminary report. *Journal of the American Medical Association* **127:**639-642.

Haslam IS, O'Reilly DA, Sherlock DJ, Kauser A, Womack C, and Coleman T (2011) Pancreatoduodenectomy as a source of human small intestine for Ussing chamber investigations and comparative studies with rat tissue. *Biopharmaceutics & drug disposition* **32:**210-221.

Higuchi W, Ho N, Park J, and Komiya I (1981) Rate-limiting steps and factors in drug absorption. *Drug Absorption* **1981:**35-60.

Ho NF, Park JY, Ni PF, and Higuchi WI (1983) Advancing quantitative and mechanistic approaches in interfacing gastrointestinal drug absorption studies in animals and humans.

Hochman JH, Chiba M, Nishime J, Yamazaki M, and Lin JH (2000) Influence of P-glycoprotein on the transport and metabolism of indinavir in Caco-2 cells expressing cytochrome P-450 3A4. *Journal of pharmacology and experimental therapeutics* **292:**310-318.

Houston JB (1994) Utility of in vitro drug metabolism data in predicting in vivo metabolic clearance. *Biochemical pharmacology* **47:**1469-1479.

Humberstone AJ and Charman WN (1997) Lipid-based vehicles for the oral delivery of poorly water soluble drugs. *Adv Drug Delivery Rev* **25:**103-128.

Inoue M, Morikawa M, Tsuboi M, Ito Y, and Sugiura M (1980) Comparative study of human intestinal and hepatic esterases as related to enzymatic properties and hydrolizing activity for ester-type drugs. *Japanese journal of pharmacology* **30:**529-535.

Johnson BM, Charman WN, and Porter CJ (2001) The impact of P-glycoprotein efflux on enterocyte residence time and enterocyte-based metabolism of verapamil. *Journal of Pharmacy and Pharmacology* **53:**1611-1619.

Johnson M, Patel DR, Matheny CJ, Ho MY, Chen L, and Ellens H (2016) Inhibition of intestinal OATP2B1 results in a significant drug-drug interaction by causing a two-fold decrease in exposure of rosuvastatin. *Drug Metabolism and Disposition***:**dmd. 116.072397.

Kato M, Chiba K, Hisaka A, Ishigami M, Kayama M, Mizuno N, Nagata Y, Takakuwa S, Tsukamoto Y, and Ueda K (2003) The Intestinal First-pass Metabolism of Substrates of CYP3A4 and P-glycoprotein—Quantitative Analysis Based on Information from the Literature. *Drug metabolism and pharmacokinetics* **18:**365-372.

Kerry NL, Somogyi AA, Mikus G, and Bochner F (1993) Primary and secondary oxidative metabolism of dextromethorphan: in vitro studies with female Sprague-Dawley and Dark Agouti rat liver microsomes. *Biochemical pharmacology* **45:**833-839.

Kim R, Leake B, Choo E, Dresser G, Kubra S, Schwarz U, Taylor A, Xie H, Stein C, and Wood A (2000) Identification of functionally important MDR1 variant alleles among African-American and Caucasian subjects. *Drug Metab Rev* **32:**199.

Kim RB, Fromm MF, Wandel C, Leake B, Wood A, Roden DM, and Wilkinson GR (1998) The drug transporter P-glycoprotein limits oral absorption and brain entry of HIV-1 protease inhibitors. *Journal of Clinical Investigation* **101:**289.

Koepsell H (1998) Organic cation transporters in intestine, kidney, liver, and brain. *Annual review of physiology* **60:**243-266.

Koo TS, Kim DH, Ahn SH, Kim KP, Kim IW, Seo SY, Suh YG, Kim DD, Shim CK, and Chung SJ (2005) Comparison of pharmacokinetics of loxoprofen and its active metabolites after an intravenous, intramuscular, and oral administration of loxoprofen in rats: evidence for extrahepatic metabolism. *Journal of pharmaceutical sciences* **94:**2187-2197.

Kool M, de Haas M, Scheffer GL, Scheper RJ, van Eijk MJ, Juijn JA, Baas F, and Borst P (1997) Analysis of expression of cMOAT (MRP2), MRP3, MRP4, and MRP5, homologues of the multidrug resistance-associated protein gene (MRP1), in human cancer cell lines. *Cancer research* **57:**3537-3547.

Kuntzman R, Lawrence D, and Conney A (1965) Michaelis constants for the hydroxylation of steroid hormones and drugs by rat liver microsomes. *Molecular pharmacology* **1:**163-167.

Kwak J-O, Lee SH, Lee GS, Kim MS, Ahn Y-G, Lee JH, Kim SW, Kim KH, and Lee MG (2010) Selective inhibition of MDR1 (ABCB1) by HM30181 increases oral bioavailability and therapeutic efficacy of paclitaxel. *European journal of pharmacology* **627:**92-98.

Lan L-B, Dalton JT, and Schuetz EG (2000) Mdr1 limits CYP3A metabolism in vivo. *Molecular pharmacology* **58:**863-869.

Lee DY, Lee MG, Shin HS, and Lee I (2007) Changes in omeprazole pharmacokinetics in rats with diabetes induced by alloxan or streptozotocin: faster clearance of omeprazole due to induction of hepatic CYP1A2 and 3A1. *Journal of Pharmacy & Pharmaceutical Sciences* **10:**420-433.

Lee JH, Noh CK, Yim CS, Jeong YS, Ahn SH, Lee W, Kim DD, and Chung SJ (2015) Kinetics of the Absorption, Distribution, Metabolism, and Excretion of Lobeglitazone, a Novel Activator of Peroxisome Proliferator-Activated Receptor Gamma in Rats. *Journal of Pharmaceutical sciences* **104:**3049-3059.

Lee Y-J, Chung S-J, and Shim C-K (2005) Limited role of P-glycoprotein in the intestinal absorption of cyclosporin A. *Biological and Pharmaceutical Bulletin* **28:**760-763.

Leyden JJ (1985) Absorption of minocycline hydrochloride and tetracycline hydrochloride: effect of food, milk, and iron. *Journal of the American Academy of Dermatology* **12:**308-312.

Li LY, Amidon GL, Kim JS, Heimbach T, Kesisoglou F, Topliss JT, and Fleisher D (2002) Intestinal metabolism promotes regional differences in apical uptake of indinavir: coupled effect of P-glycoprotein and cytochrome P450 3A on indinavir membrane permeability in rat. *Journal of Pharmacology and Experimental Therapeutics* **301:**586-593.

Lin JH (1999) Role of pharmacokinetics in the discovery and development of indinavir. *Advanced drug delivery reviews* **39:**33-49.

Lin JH, Chen I-W, Vastag KJ, and Ostovic D (1995) pH-dependent oral absorption of L-735,524, a potent HIV protease inhibitor, in rats and dogs. *Drug metabolism and disposition* **23:**730-735.

Lin JH, Chiba M, and Baillie TA (1999a) Is the role of the small intestine in first-pass metabolism overemphasized? *Pharmacological reviews* **51:**135-158.

Lin JH, Chiba M, Balani SK, Chen I-W, Kwei G, Vastag KJ, and Nishime JA (1996) Species differences in the pharmacokinetics and metabolism of indinavir, a potent human immunodeficiency virus protease inhibitor. *Drug metabolism and disposition* **24:**1111-1120.

Lin JH, Chiba M, Chen I-W, Nishime JA, Yamazaki M, and Lin YJ (1999b) Effect of dexamethasone on the intestinal first-pass metabolism of indinavir in rats: evidence of cytochrome P-450 A and P-glycoprotein induction. *Drug metabolism and disposition* **27:**1187-1193.

Müller M and Jansen PL (1998) The secretory function of the liver: new aspects of hepatobiliary transport. *Journal of hepatology* **28:**344-354.

Meijer D, Smit J, and Müller M (1997) Hepatobiliary elimination of cationic drugs: the role of P-glycoproteins and other ATP-dependent transporters. *Advanced drug delivery reviews* **25:**159-200.

Mouly SJ, Paine MF, and Watkins PB (2004) Contributions of CYP3A4, P-glycoprotein, and serum protein binding to the intestinal first-pass

extraction of saquinavir. *Journal of Pharmacology and Experimental Therapeutics* **308:**941-948.

Murakami T and Takano M (2008) Intestinal efflux transporters and drug absorption. *Expert Opinion on Drug Metabolism & Toxicology* **4:**923-939.

Naritomi Y, Terashita S, Kimura S, Suzuki A, Kagayama A, and Sugiyama Y (2001) Prediction of human hepatic clearance from in vivo animal experiments and in vitro metabolic studies with liver microsomes from animals and humans. *Drug metabolism and Disposition* **29:**1316-1324.

Oostendorp RL, Buckle T, Beijnen JH, van Tellingen O, and Schellens JH (2009) The effect of P-gp (Mdr1a/1b), BCRP (Bcrp1) and P-gp/BCRP inhibitors on the in vivo absorption, distribution, metabolism and excretion of imatinib. *Investigational new drugs* **27:**31-40.

Paek IB, Ji HY, Kim MS, Lee G, and Lee HS (2006a) Metabolism of a new P-glycoprotein inhibitor HM-30181 in rats using liquid chromatography/electrospray mass spectrometry. *Rapid communications in mass spectrometry* **20:**1457-1462.

Paek IB, Ji HY, Kim MS, Lee GS, and Lee HS (2006b) Simultaneous determination of paclitaxel and a new P-glycoprotein inhibitor HM-30181 in rat plasma by liquid chromatography with tandem mass spectrometry. *Journal of separation science* **29:**628-634.

Paek IB, Kim SY, Kim MS, Kim J, Lee G, and Suk Lee H (2007) Characterization of Human Liver Cytochrome P-450 Enzymes Involved in the O-demethylation of a New P-glycoprotein Inhibitor HM-30181∗. *Journal of Toxicology and Environmental Health, Part A* **70:**1356-1364.

Paulson SK, Vaughn MB, Jessen SM, Lawal Y, Gresk CJ, Yan B, Maziasz TJ, Cook CS, and Karim A (2001) Pharmacokinetics of celecoxib after oral administration in dogs and humans: effect of food and site of

absorption. *Journal of Pharmacology and Experimental Therapeutics* **297:**638-645.

Press B (2011) Optimization of the Caco-2 permeability assay to screen drug compounds for intestinal absorption and efflux, in: *Permeability Barrier*, pp 139-154, Springer.

Putnam WS, Ramanathan S, Pan L, Takahashi LH, and Benet LZ (2002) Functional characterization of monocarboxylic acid, large neutral amino acid, bile acid and peptide transporters, and P-glycoprotein in MDCK and Caco-2 cells. *Journal of pharmaceutical sciences* **91:**2622-2635.

Rouquayrol M, Gaucher B, Roche D, Greiner J, and Vierling P (2002) Transepithelial transport of prodrugs of the HIV protease inhibitors saquinavir, indinavir, and nelfinavir across Caco-2 cell monolayers. *Pharmaceutical research* **19:**1704-1712.

Sekine T, Cha SH, Kanai Y, and Endou H (1999) Molecular biology of multispecific organic anion transporter family (OAT family). *Clinical and Experimental Nephrology* **3:**237-243.

Senior JR (1964) Intestinal absorption of fats. *Journal of lipid research* **5:**495-521.

Spahn-Langguth H and Langguth P (2001) Grapefruit juice enhances intestinal absorption of the P-glycoprotein substrate talinolol. *European journal of pharmaceutical sciences* **12:**361-367.

Tam D, Sun H, and Pang KS (2003) Influence of P-glycoprotein, transfer clearances, and drug binding on intestinal metabolism in Caco-2 cell monolayers or membrane preparations: a theoretical analysis. *Drug metabolism and disposition* **31:**1214-1226.

Tamai I, Nezu J-i, Uchino H, Sai Y, Oku A, Shimane M, and Tsuji A (2000) Molecular identification and characterization of novel members of the human organic anion transporter (OATP) family. *Biochemical and biophysical research communications* **273:**251-260.

Thummel KE, Kunze KL, and Shen DD (1997) Enzyme-catalyzed processes of first-pass hepatic and intestinal drug extraction. *Advanced drug delivery reviews* **27:**99-127.

van Waterschoot RA and Schinkel AH (2011) A critical analysis of the interplay between cytochrome P450 3A and P-glycoprotein: recent insights from knockout and transgenic mice. *Pharmacological reviews* **63:**390-410.

Varma MV, Sateesh K, and Panchagnula R (2005) Functional role of P-glycoprotein in limiting intestinal absorption of drugs: contribution of passive permeability to P-glycoprotein mediated efflux transport. *Molecular pharmaceutics* **2:**12-21.

Wacher VJ, Silverman JA, Zhang Y, and Benet LZ (1998) Role of P-glycoprotein and cytochrome P450 3A in limiting oral absorption of peptides and peptidomimetics. *Journal of pharmaceutical sciences* **87:**1322-1330.

Watkins PB (1997) The barrier function of CYP3A4 and P-glycoprotein in the small bowel. *Advanced drug delivery reviews* **27:**161-170.

Yoon I-S, Choi M-K, Kim JS, Shim C-K, Chung S-J, and Kim D-D (2011) Pharmacokinetics and first-pass elimination of metoprolol in rats: contribution of intestinal first-pass extraction to low bioavailability of metoprolol. *Xenobiotica* **41:**243-251.

Zhang L, Lin G, Chang Q, and Zuo Z (2005) Role of intestinal first-pass metabolism of baicalein in its absorption process. *Pharmaceutical research* **22:**1050-1058.

TABLE 1

Summary of the model input parameters. In this study, K_m value of rat enzyme (Cyp3a) was assumed to be comparable to that of human enzyme (CYP3A4)(Hochman et al., 2000). MPPGG (i.e., milligram protein per gram gut) was considered to be 15.5 in this study.

Parameters	Units	Values
P_{app}	cm/s	4.34×10^{-6}
S	cm^2	0.636
$PS_1,\ PS_2$	mL/min	3.31×10^{-4}
K_m	μM	2.5
V_{max}	nmol/min/mg protein	1.54×10^{-4}
CL_m	V_{max}/K_m	
$K_{m,P-gp}$	μM	140
$V_{max,P-gp}$	nmol/min/mg protein	0.201
CL_{eff}	$V_{max,P-gp}/K_{m,P-gp}$	
V_D	mL	2
V_C	mL	0.07
V_A	mL	2

TABLE 2

Elimination rate constant and apparent clearance of CYP substrates in the presence and the absence of HM-30181A in rat liver microsomes (n = 4)

Phenotype	Substrate	Control		(+) HM-30181A	
		K_{el}	CL_{int}	K_{el}	CL_{int}
		min^{-1}	mL/min/kg	min^{-1}	mL/min/kg
1A2	Phenacetin	0.0035 ± 0.0006	12.6 ± 2.1	0.0038 ± 0.0005	13.5 ± 1.8
2C9	Diclofenac	0.0247 ± 0.0006	88.8 ± 2.1	0.0237 ± 0.0025	85.2 ± 9.1
2C19	Omeprazol	0.0940 ± 0.0026	338 ± 10	0.0923 ± 0.0031	332 ± 11
2D6	Dextromethorphan	0.0830 ± 0.0053	299 ± 19	0.0783 ± 0.0022	282 ± 8
3A4	Testosterone	0.213 ± 0.031	716 ± 55	0.209 ± 0.029	752 ± 105

K_{el}, elimination rate constant; CL_{int}, microsomal intrinsic clearance

TABLE 3

Cellular accumulation rate of substrates in transfected MDCKII/FRT cells.

Expressing transporter	Substrate	Accumulation of substrate in % of control	
		(+) HM-30181A	(+) Reference inhibitor*
rOatp1b2	[^{3}H] estrone-3-sulfate	123 ± 25	64.6 ± 14.1
rOat1	[^{3}H] ρ-aminohippuric acid	105 ± 10	17.9 ± 5.1
rOat3	[^{3}H] estrone-3-sulfate	107 ± 5	55.0 ± 7.6
rOct2	[^{3}H] 1-methyl-4phenylpyridium	102 ± 6	8.8 ± 0.3

* atorvastatin for rOatp1b2, probenecid for rOat1 and rOat3, diphenhydramine for rOct2

TABLE 4

Summary of pharmacokinetic parameters for indinavir and M6 after intravenous, oral and portal vein administration in the presence and the absence of HM-30181A co-administration in rats (n = 4 or 5)

		indinavir		M6	
		control	*(+) HM-30181A*	*control*	*(+) HM-30181A*
Intravenous injection (1 mg/kg)					
$T_{1/2}$	*min*	51.3 ± 21.1	50.7 ± 13.0		
CL	*mL/min/kg*	112 ± 16.1	82.3 ± 3.5		
V_{ss}	*L/kg*	4.74 ± 2.33	3.48 ± 0.79		
AUC	*min*μg/mL*	9.08 ± 1.33	11.3 ± 4.1		
Intravenous injection (10 mg/kg)					
$T_{1/2}$	*min*	30.5 ± 4.1	29.5 ± 12.0		
CL	*mL/min/kg*	72.7 ± 7.2	63.4 ± 21.0		
V_{ss}	*L/kg*	2.86 ± 0.22	2.20 ± 0.53		
AUC	*min*μg/mL*	139 ± 14	168 ± 43	6.38 ± 0.79	7.38 ± 1.38
T_{max}	*min*			15.0 ± 0.0	15.0 ± 0.0
C_{max}	*μg/mL*			0.0964 ± 0.0282	0.0992 ± 0.0280
Oral administration (10 mg/kg)					
AUC	*min*μg/mL*	25.3 ± 2.6	53.4 ± 20.9*	2.64 ± 0.27	5.28 ± 2.13*
T_{max}	*min*	20.0 ± 0.0	17.5 ± 2.9	24.0 ± 4.2	22.5 ± 2.9
C_{max}	*μg/mL*	0.614 ± 0.083	1.51 ± 0.64*	0.0477 ± 0.0083	0.114 ± 0.048*
Portal vein infusion (5 mg/kg)					
AUC	*min*μg/mL*	51.6 ± 14.4	127 ± 31*	3.17 ± 0.93	6.08 ± 1.51*
T_{max}	*min*	20.0 ± 0.0	20.0 ± 0.0	28.3 ± 2.9	48.3 ± 36.2
C_{max}	*μg/mL*	1.56 ± 0.31	2.22 ± 0.98	0.0882 ± 0.0124	0.109 ± 0.005

$T_{1/2}$, half-life; CL, clearance; V_{ss}, steady state volume of distribution; AUC, area under the curve; T_{max}, time point at maximum concentration; C_{max}, maximum concentration

* $p < 0.05$ significance between control and HM-30181A by two-tailed unpaired t-test

TABLE 5

Apparent permeability and accumulation of indinavir and M6 in rat intestinal tissue (n = 5)

	P_{app}	amount in tissue	
	indinavir	indinavir	M6
	10^{-6} cm/sec	*pmole/g tissue*	
Control	2.85 ± 0.19	2650 ± 1130	54.9 ± 10.9
(+) HM-30181A	4.34 ± 1.08*	3290 ± 1110	77.3 ± 16.3*

P_{app}, apparent permeability

* $p < 0.05$ significance between control and HM-30181A group by two-tailed unpaired t

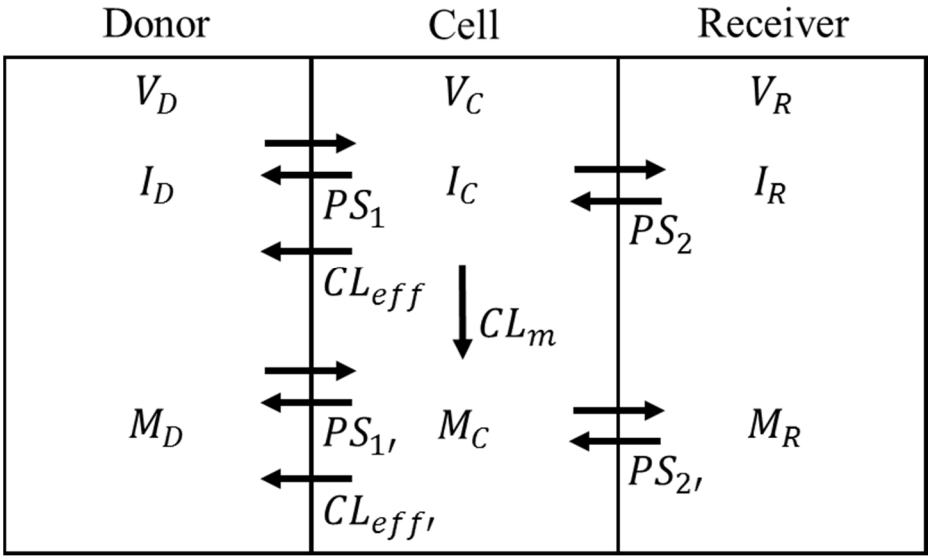

Fig. 1. Kinetic model for ex vivo results on intestinal metabolism to M6 and transport of indinavir

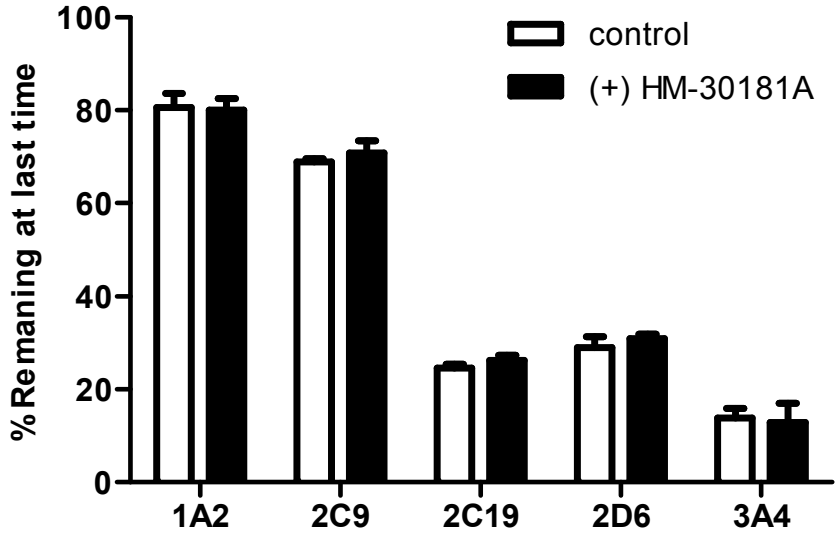

Fig. 2. The amount remaining CYP substrate in percent of the initial amount in the last sampling time in rat liver microsomes. The activity of CYP enzyme was examined in the absence (open bar) and the presence (solid bar) of HM-30181A. Values are expressed as the mean ± S.D. of n = 4

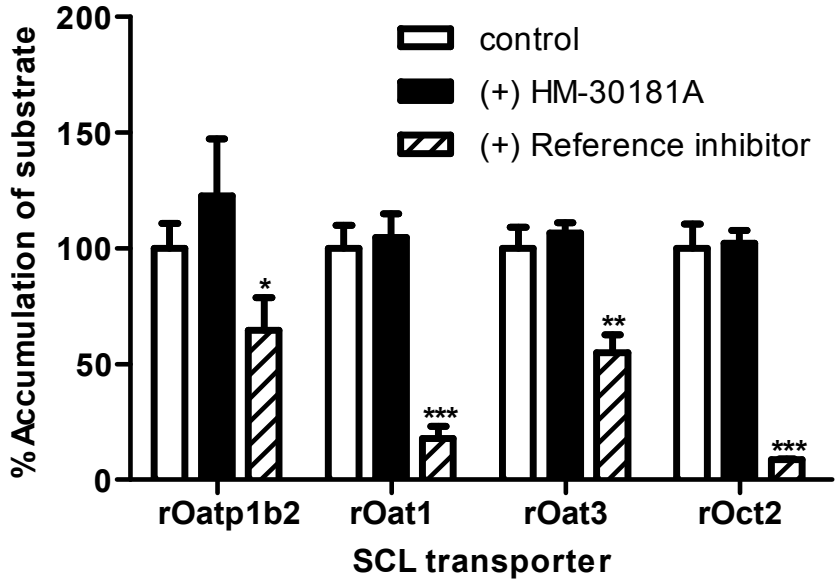

Fig. 3. Cellular accumulation of corresponding substrates in transporter transfected MDCKII/FRT cells. [^{3}H] estrone-3-sulfate (E3S; rOatp1b2 and rOat3), [^{3}H] p-aminohippuric acid (PAH; rOat1) and [^{3}H] 1-methyl-4phenylpyridium (MPP+; rOct2) were examined in the absence (open bar) and the presence (solid bar) of HM-30181A or reference inhibitors (diagonal bar; atorvastatin, probenecid or diphenhydramine). Values are expressed as the mean ± S.D. of n = 4. Key: * $p < 0.05$, ** $p < 0.01$ and *** $p < 0.001$ in comparison to control.

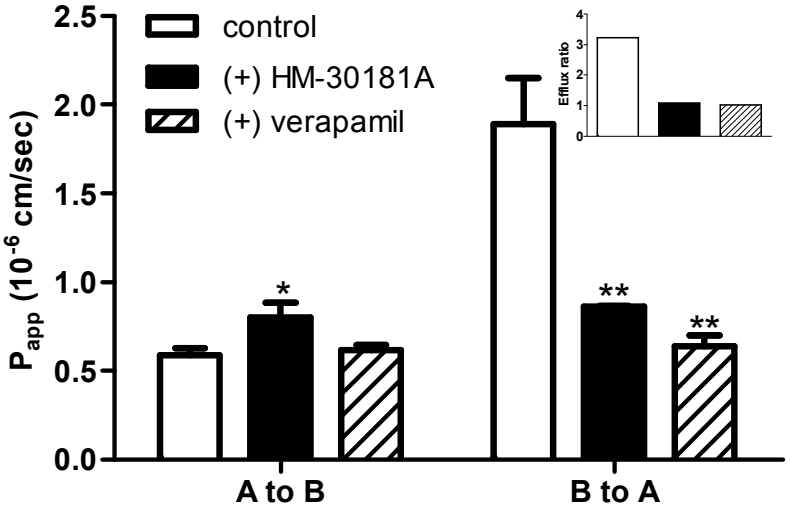

Fig. 4. Apparent permeability and efflux ratio of M6 in the absence (open bar), and the presence of (solid bar) HM-30181A or verapamil (i.e., reference P-gp inhibitor; diagonal bar) in Caco-2 cell monolayers. The apparent permeability of M6 from the apical to basolateral side was 0.586 ± 0.039, 0.800 ± 0.085 and 0.615 ± 0.030 x 10^{-6} cm/sec for control, (+) HM-30181A and (+) verapamil group, respectively. The apparent permeability of M6 from the basolateral to apical side was 1.89 ± 0.26, 0.864 ± 0.002 and 0.636 ± 0.062 x 10^{-6} cm/sec for control, (+) HM-30181A and (+) verapamil group. Estimated efflux ratio for M6 was 3.23, 1.08 and 1.03 for control, (+) HM-30181A and (+) verapamil, respectively. Values are expressed as the mean ± S.D. of n = 3. Key: * $p < 0.05$ and ** $p < 0.01$ in comparison to control.

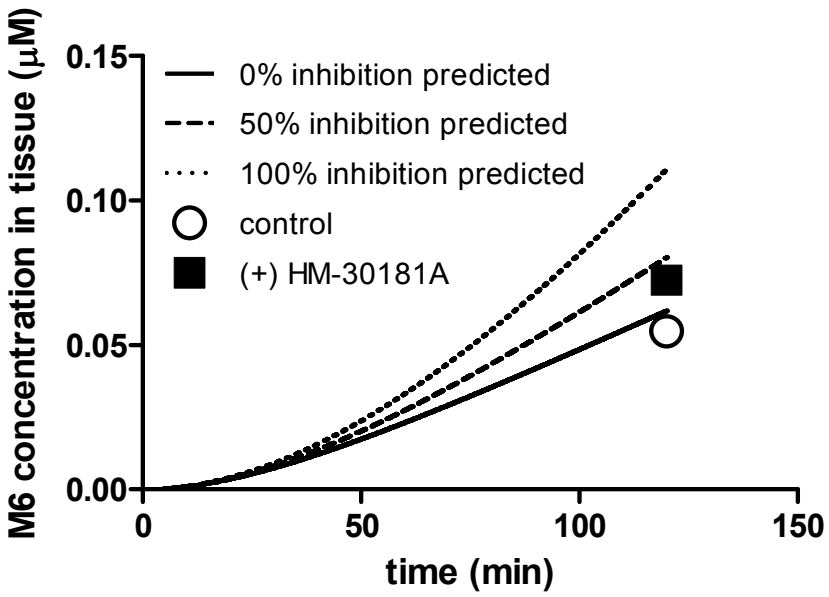

Fig. 5. Simulated effect of P-gp efflux on the metabolism of indinavir in intestinal tissue. Symbols in the figure represents the observation in ex vivo studies and the lines are generated from the kinetic model (Fig 1, eq. 1~6)

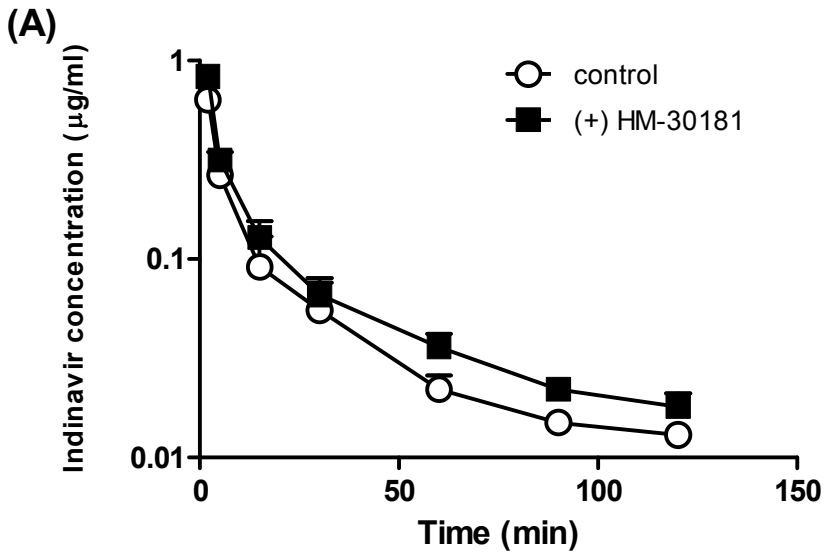
(A)
Indinavir concentration (μg/ml)
1
0.1
0.01
0
50
100
150
Time (min)
control
(+) HM-30181

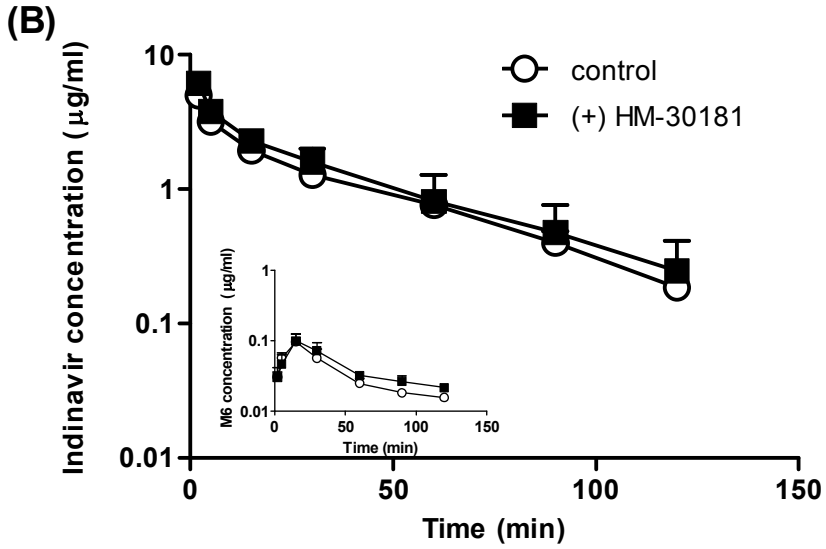
(B)
Indinavir concentration (μg/ml)
10
1
0.1
0.01
0
50
100
150
Time (min)
control
(+) HM-30181
M6 concentration (μg/ml)
1
0.1
0.01
0
50
100
150
Time (min)

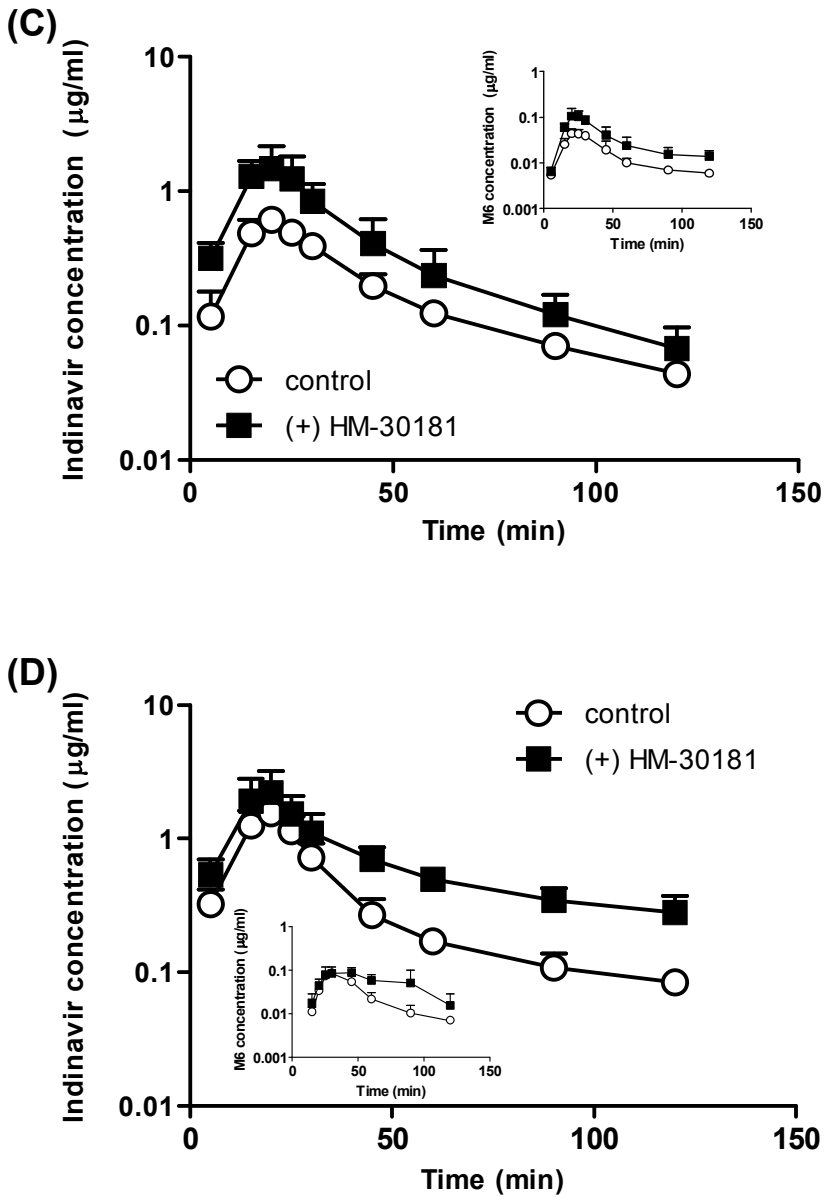

Fig. 6. Plasma concentration of indinavir and M6 (in-set) in the absence (open circle) or the presence (solid square) of HM-30181A co-administration. Key: (A), 1 mg/kg intravenous injection; (B), 10 mg/kg intravenous injection; (C), 10 mg/kg oral administration; (D), 5 mg/kg portal vein infusion. Values are expressed as the mean ± S.D. of n = 4 or 5

6. Appendix

Pharmacokinetics of HM-30181A after a single oral dose of 10 mg/kg in rats.

The surgical procedure were described in the main text. Rats (n = 4) received a single oral dose of HM-30181A (DMAc:PEG400:saline = 1:2:1, v/v/v) at 10 mg/kg (administration volume of 2 mL/kg). Approximately 150 μL of blood was collected at 0, 5, 10, 20, 30, 60, 90, 120, 180, 240, 480 and 1440 min. Blood samples were immediately centrifuged at 16,100 g for 10 minutes (4℃), and the supernatants were collected / stored at -20℃ until the analysis for the inhibitor by LC-MS/MS. To determine the hepatic concentration of HM-30181A, rats received a single oral dose of 10 mg/kg (n=4). The animal was then sacrificed at 10, 30 and 130 min after the dose and the liver was immediately dissected. The tissue was homogenized in a 2-fold volume of DPBS with a homogenizer (Ultra Turrax model, T25, IKA Works, Inc., Cincinnati, OH). The tissue homogenate (50 μL) was added with 200 μL acetonitrile for deproteination. All samples were then vortexed for 10 minutes and centrifuged at 16,100 g at 4℃ for 5 min. The supernatant was collected and the aliquot (5 μL) injected onto LC-MS/MS system. In this study, glipizide (100 ng/mL) was used as the internal standard and the compound was added to acetonitrile used for the deproteination. The mobile phases consisted of (A) 0.1% formic acid in acetonitrile and (B) 0.1% formic acid in water. The flow was delivered at the flow rate of 0.3 mL/min with a

gradient (i.e., mobile phase (A), 50%-0.5 min, 90%-0.6 min, 90%-1.0 min, 75%-1.1 min, 75%-3.0 min, 50%-3.1 min, 50%-5.0 min). In this study, a reverse phase HPLC column [i.e., Eclipse XDB-C18, 3.5 μm, 2.1 X 100 mm (Agilent Technologies, Santa Clara, CA)] was used. The samples were ionized using turbo ion spray interface in the positive ionization mode and monitored at the following Q1/Q3 transitions (m/z): 688.9/541.0 for HM-30181A and 445.8/320.9 for glipizide. The common source/gas of HM-30181A and glipizide was as follows: The ion spray voltage, source temperature and pressure of the curtain gas were 5500 V, 500°C and 10 psi. The ion source gas1 and gas2 were 30 and 40 psi, respectively. The declustering potential (DP) for HM-30181A and glipizide were 36.0 and 47.5 V, respectively. The entrance potential (EP) were 5.7 and 4.02 V, collision energy (CE) were 30.4 and 17 V and the collision cell exit potential (CXP) were 7.6 and 8.0 V, respectively. Calibration standard curve of HM-30181A with the concentration ranging from 10 to 5000 ng/mL, and was found linear ($R2 > 0.998$) with the intra-day accuracy from 89.6 to 110%.

The plasma concentrations of HM-30181A were below the quantification limit of the assay. In addition, the hepatic concentration was not detected at 10 min after the dosing (Table AP1). In contrast, the hepatic concentrations of HM-30181A were 37.0 ± 16.7 and 551 ± 135 pmole/g tissue after the 30 and 130 m of the administration respectively (Table AP1), suggesting that hepatic P-gp is possible for after the 30 min of the oral

administration.

Table AP1. Hepatic concentration of HM-30181A after oral dose of 10 mg/kg in rats. Mean ± S.D. (n = 4)

Time (min)	Concentration in liver (pmole/g tissue)
10	nd
30	37.0 ± 16.7
130	551 ± 135

7. 국문초록

소장 내의 efflux transporter인 P-glycoprotein(P-gp)는 기질이 소장에서 흡수되는 중에 ‘recycle’ 과정을 일으킬 수 있다. 이 연구의 목표는 약물이 소장에서 흡수될 때 초회통과를 겪으며 대사되는 과정 중 P-gp와 연관된 ‘recycling’의 기여도를 밝히는 것이다. P-gp 저해제인 HM-30181A과 CYP 효소들(1A2, 2C9, 2C19, 2D6, 3A4)의 상관관계를 확인하기 위하여, HM-30181A의 존재 여부에 따라 각 CYP 효소들의 지표가 되는 기질들의 안정성을 랫드의 간 마이크로좀을 이용한 in vitro 실험에서 수행하였다. 또한 대표적인 SCL transporter들(rOatp1b2, rOat1, rOat3, rOct2)과의 상관관계를 알아보기 위하여 각 수송체가 발현된 MDCKII/FRT cell에서의 표준 기질에 대한 uptake를 HM-30181A를 병용 처리하여 확인하였다. 이 연구의 모델 물질은 P-gp와 CYP3A4의 공통 기질이자 protease 저해제로 잘 알려진 indinavir를 선정하였다. 랫드에 10 mg/kg의 HM-30181A를 경구로 10분 먼저 투여한 후, indinavir를 10 mg/kg의 양으로 경구 투여하였다. 간문맥 등속 주입 실험에서는 대조군과 실험군 랫드의 간문맥에 catheter를 삽입하고 이를 통하여 15 mg/kg/h로 20분 간 indinivir를 등속 주입하였으며 저해제는 10분 먼저 경구투여하였다. HM-30181은 대표적인 CYP 효소들(1A2, 2C9, 2C19, 2D6, 3A4)과 SLC 수송체들(rOatp1b2, rOat1, rOat3, rOct2)의

활동에 영향을 미치지 않았다. 이를 통하여 HM-30181은 P-gp에 특정한 저해제임을 확인할 수 있었다. 경구투여 실험에서 indinavir의 C_{max} ($C_{max,\ IND}$)은 대조군과 실험군에서 각각 0.614 ± 0.083과 1.51 ± 0.64 μg/mL이었다. Indinavir의 AUC (AUC_{IND}) 또한 비슷한 결과를 나타내었다. 즉, HM-30181 처리군이 대조군보다 AUC가 약 111% 높았다 ($p<0.05$). 주대사체인 M6의 AUC (AUC_{M6}) 또한 AUC_{IND}에서와 비슷한 경향의 증가를 보였다. 간문맥 등속 주입 실험에서는 HM-30181 처리군에서 $C_{max,\ IND}$, AUC_{IND}, AUC_{M6}가 각각 1.4, 2.5, 1.9배가 증가하였다. Ussing chamber 실험에서 겉보기 투과계수(P_{app})는 대조군과 HM-301781을 처리한 실험군에서 각각 2.85 ± 0.19와 4.34 ± 1.08 X 10^{-6} cm/sec를 나타내었다. 소장 조직내의 indinavir의 누적양은 비록 통계학적으로 유의미한 차이를 보이지 않았으나 대조군과 실험군에서 각각 2650 ± 1130, 3290 ± 1110 pmole/g tissue로 증가하는 경향을 나타내었다. M6의 누적양은 각각 54.9 ± 10.9, 77.3 ± 16.3 pmole/g tissue로 HM-30181A를 처리한 경우 뚜렷한 증가($p < 0.05$)를 보였으며, recycling과 대사를 함께 가정한 동태학 모델을 통한 simulation 결과와도 동일한 양상를 나타내었다. 따라서, indinavir의 여러 경로투여를 통한 in vivo study, ex vivo study 그리고 in silico study를 모두 종합해 보았을 때, HM-30181A에 의해 indinavir의 흡수와 대사는 약간 증가하는 경향을 보인다고 할 수 있다.

주요어: P-glycoprotein; 재흡수; 초회통과 효과; indinavir; HM-30181A

PART II

Quantification of EC-18,

a synthetic monoacetyldiglyceride

(1-palmitoyl-2-linoleoyl-3-acetyl-rac-glycerol),

in rat and mouse plasma by

liquid-chromatography/tandem mass spectrometry

1. Introduction

Cancer chemotherapy is often associated with a host of adverse effects, including neutropenia. This dose limiting toxicity typically causes a decrease in leukocyte and neutrophil counts resulting in the incidence of infections such as pneumonia and sepsis in patients to be significantly elevated [1, 2]. As a standard therapy for this condition, granulocyte colony-stimulating factor is administered to patients receiving chemotherapy, although the treatment does not fully prevent the development of fevers and/or infections in immunocompromised subjects, especially elderly, patients [3, 4].

1-Palmitoyl-2-linoleoyl-3-acetyl-rac-glycerol (EC-18), a monoacetyldiglyceride, was originally isolated from antlers of the Sika deer (Cervus nippon Temminck) [5]. Although monoacetyldiglycerides are typically found in food, EC-18 can now be chemically synthesized in high yields by reacting glycerol, palmitic acid, and linoleic acid [6]. Rockpid®, a functional food product, contains EC-18 as the principal ingredient and was recently approved by Korean FDA. A literature search indicated that the compound was previously reported to stimulate the proliferation of hematopoietic stem cells and bone marrow stromal cells in vitro/in vivo, and to inhibit hematogenous metastasis in of biliary cancer cells in a hamster model [5, 7]. Furthermore, EC-18 may modulate eosinophil chemotaxis in

epithelial cells, and effectively suppress neutrophilic inflammation [8, 9]. In short, the compound is expected to be clinically useful for controlling / ameliorating conditions caused by inflammations. It was recently reported that the United States FDA approved phase II clinical trials of EC-18 for the management of severe chemotherapy-induced neutropenia in patients with advanced breast cancer who are receiving intermediate febrile neutropenia risk chemotherapy.

The absorption of glycerol and glycerides, probably EC-18 as well, proceed via complicated mechanism(s), as evidenced by their rapid decomposition during the digestion / absorption processes [10]. Furthermore, they may also be rapidly cleared by esterase enzymes that are produced in the body [11], suggesting that these compounds are likely to have a low bioavailability and short half-life. Therefore, protective formulation(s) that guarantee(s) the stability in the intestine and in the body may be necessary [12, 13]. Despite the fact a number of studies regarding the pharmacological mechanism(s) of EC-18 have appeared in the literature, however, the pharmacokinetics and the mechanisms responsible for the absorption/elimination of EC-18 remains unknown. Therefore, the objective of this study was to develop and validate an analytical methodology according to guidelines set by the FDA [22] for the quantification of EC-18 in plasma samples obtained from small animal models. We were particularly interested in testing the applicability of the current method to pharmacokinetic studies involving small animals, since these animal models are likely to be useful in

the early development of formulation for the compound. The findings indicate that the assay is capable of detecting EC-18 down to 50 ng/mL in rat and mouse plasma samples using only a limited sample size (50 µL), which will permit the method to be used in pharmacokinetic studies involving small animals.

2. Material and Method

2.1. Chemicals and reagents

EC-18 (98.7% purity) and EC-18-d3 [an internal standard (IS)] were kindly provided by EnzyChem Lifesciences Co. (Seoul, Korea). Methanol (HPLC grade) and isopropyl alcohol (IPA, HPLC grade) were obtained from Fisher Scientific (Pittsburgh, PA). Formic acid (FA) was purchased from Sigma-Aldrich (St. Louis, MO). Blank rat and mouse plasma samples containing heparin (an anticoagulant) were obtained from Orient Bio Inc. (Gyeonggi-do, Korea).

2.2. LC conditions

In this study, an HPLC system [Waters e2695 HPLC system (Milford, MA)], consisting of a binary pump, an online degasser, an autosampler, a column heater, and a reversed phase HPLC column [Synergi 4 μm Polar-RP 80 Å LC Column (150 mm × 2 mm, Phenomenex, Torrance, CA)] was used for chromatographic separations. The mobile phase A and B were composed of MeOH-IPA-FA (60:40:0.1, v/v/v) and 0.1% (v/v) FA in purified water, respectively. The flow rate of the mobile phase at 0.3 mL/min and the sample volume of 5 μ5 were used in this study. The analytical samples and column were maintained at 4˚C and 30˚C, respectively.

2.3. Mass spectrometer conditions

Mass spectrometric detection was performed with an API 3200 QTrap (Applied Biosystems, Foster City, CA), equipped with an electro-spray ionization (ESI) source operating in the positive-ion mode. In this study, the multiple reaction monitoring (MRM) method was used to detect the analytes: The MRM m/z transitions were monitored at 635.4→355.4 for EC-18 and 638.4→338.4 for the IS. The ion spray voltage, source temperature and pressure of the curtain gas were 5000 V, 200°C and 10 psi, respectively. The declustering potentials for EC-18 and IS were 20 and 101 V, the entrance potentials were 10 and 6.5 V, respectively. The collision energies were 30 and 51 V, and collision cell exit potential were 6.0 and 4.0 V, respectively. In this study, data acquisition and processing were performed with the Analyst™ software (version 1.4.2; Applied Biosystems) running on a PC.

2.4. Standards and quality control (QC) samples

Stock solutions of EC-18 and IS were prepared in MeOH containing 0.1% (v/v) FA at concentrations of 1000 μg/mL and 1000 ng/mL, respectively. A batch of EC-18 standard solutions and QC solutions was prepared by the serial dilution of the stock solutions with MeOH containing 0.1% FA (v/v). A 5 μL aliquot of an EC-18 standard solution was added to 45 μL of blank rat or mouse plasma for the preparation of calibration standards containing EC-18 at 50, 100, 250, 500, 1000, 2500, 5000 or 10000 ng/mL. Using a similar dilution

method, a batch of QC samples was prepared so as to have concentrations of EC-18 at 50, 150, 1000, and 8000 ng/mL in blank plasma. The samples were then processed similar to the procedure described in section 2.5 (see below).

2.5. Sample preparation

A 50 µL aliquot of plasma sample was transferred to a SafeSeal Microcentrifuge Tube (Sorenson BioScience, Inc., Murray, UT). A 200 µL aliquot of IS solution (200 ng/mL in MeOH containing 0.1% FA, v/v) was added to the sample, followed by vortexing for 10 min. The mixture was then centrifuged at 16,100 g at 4°C for 10 min and the supernatant transferred to an analysis vial. A 5 µL aliquot was injected onto the LC-MS/MS system.

2.6. Method validation

2.6.1. Selectivity

In this study, six lots of plasma samples from six different rats/mice were prepared to evaluate the selectivity of the assay. In particular, the presence of any interfering peak in double blank samples (i.e., samples without EC-18 and without IS), blank samples (i.e., blank plasma added with the IS only) and the lower limit of quantification (LLOQ) for the samples was carefully monitored.

2.6.2. Linearity

Calibration curves, in the concentration range from 50 to 10000 ng/mL, were constructed with the ratios of the peak area of EC-18 to that of the IS against the EC-18 concentration in the plasma standards. The calibration curves were fitted using a linear regression model with intercept and weighing factor of 1/standard concentration for the data.

2.6.3. Precision, accuracy and dilution

Three batches were prepared on different days to determine the precision and accuracy of the assay. Each batch consisted of six replicates of QC samples at concentrations of 150, 1000 and 8000 ng/ml and LLOQ samples (50 ng/mL). Another batch was prepared with six replicate samples containing 80000 ng/mL and diluted tenfold with blank plasma to give the expected concentration at 8000 ng/mL. All samples were then processed according to the procedure described in the previous section.

The precision was determined as the percent coefficient of variation at each concentration. The accuracy was estimated by calculating the percent difference between the calculated and theoretical concentrations.

2.6.4. Matrix effect and recovery

The absolute/relative matrix effect and recoveries of EC-18 and IS were assessed by analyzing three sets of standards at three concentrations (i.e., 150, 1000, and 8000 ng/mL). To determine the adequate medium for deproteination/extraction between MeOH and ACN, the recovery study was

conducted in rats and mice plasma: There was no difference in extraction between the solvents (Supplement 3). In subsequent studies, therefore we chose to use MeOH as extraction solvent. To determine the absolute matrix effect for EC-18 and IS, samples of blank blood obtained from six different rats or mice were extracted as described previously, and EC-18 and IS were added to the post-extraction sample to generate three concentrations (set 2). The mean peak areas of the analyte were compared with the mean peak areas from neat solutions of the analyte in a MeOH solution containing 0.1% formic acid (set 1). In the case of the relative matrix effect, the variability, expressed as precision (CV, %), in the peak areas for the analyte that had been added to the post-extraction samples from the blank blood of six different rats or mice (set 2) was determined and was considered to be the relative matrix effect [14].

The recoveries of EC-18 and IS were determined by comparing the mean peak areas of analytes added before extraction to the same six different sources (set 3) with those of the analytes added to the post-extraction samples from different lots of rats and mice plasma at the same three concentrations (set 2).

2.6.5. Stability

To determine the stability of EC-18 under typical conditions in laboratories, the stability of EC-18 in stock solutions was examined at room temperature for 6 h, in refrigerated storage conditions (4°C) for 24 h and 2 weeks, and in two frozen conditions (–20°C and –80°C) for 2 weeks. In

addition, the stability of EC-18 in the QC samples (i.e., 150, 1000 and 8000 ng/mL) was examined for four different conditions, as follows: QC samples stored at room temperature for 24 h, samples that had been processed (i.e., post-preparative stability) at 4°C for 3 days, samples that were subjected to 3 freeze-thaw cycles, and the samples that had been subjected to long-term storage (–80°C) for 2 weeks. Analytes were considered to be stable when the measured concentrations did not deviate from theoretical concentrations by more than 15%.

2.7. Application to pharmacokinetic study of EC-18

To determine whether the current assay method is applicable to pharmacokinetic characterization studies for EC-18, the monoacetyldiglyceride was administered to rats / mice via intravenous or oral administration. In this study, the dose of EC-18 via intravenous and oral administration was 1 and 2000 mg/kg in rats, and 5 and 2000 mg/kg in mice, respectively. Male Sprague–Dawley rats, weighing 245 to 250 g, and ICR mice, weighing 23 to 25 g, were used in this study. Experimental protocols involving the animals used in this study were reviewed by Seoul National University Institutional Animal Care and Use Committee according to the National Institutes of Health Publication Number 85-23 Principles of Laboratory Animal Care revised in 1985. EC-18 was dissolved in saline containing 3% Tween 80 and the solution administrated via the intravenous route (volume of administration, 1 mL/kg for rats; 2 mL/kg for mice). In the

oral administration study, EC-18 was administrated in the original oil form (volume of administration, 2 mL/kg for rats; 2 mL/kg for mice). Blood samples (150 μL) were collected in heparinized tubes via the right femoral artery at 0, 2, 5, 10, 15, 30, 60, 90, 120, 240, and 480 min after being administered to rats. For the pharmacokinetic study involving mice, blood samples (200 μL) were collected via retro-orbital plexus in both the intravenous and oral administration study at 0, 5, 15, 30, 60, 120, 240, 360 or 480 min and 0, 15, 30, 60, 120, 240, 360, 480, 720 or 1440 min, respectively. Plasma samples, obtained by centrifugation of the blood at 16,100 g for 10 min, were collected and stored at –80°C prior to analysis. The plasma concentration versus time data for EC-18 was analyzed by the non-compartmental method using the WinNonlin software (Ver. 3.1; Pharsight, Mountain View, CA, USA) running on a PC. The area under the EC-18 concentration in the plasma-time curve from time zero to infinity ($AUC_{0\rightarrow\infty}$) and the area under the respective first moment−time curve from time zero to infinity ($AUMC_{0\rightarrow\infty}$) were calculated by the linear trapezoidal method and the standard area extrapolation method [16]. The mean residence time (MRT) was calculated $AUMC_{0\rightarrow\infty}$ divide by $AUC_{0\rightarrow\infty}$. In this study, a standard moment analysis was applied to calculate systemic clearance (CL), half-life ($T_{1/2}$) and steady-state volume of distribution (V_{ss}). The maximum EC-18 concentration (C_{max}) and the time point at C_{max} (T_{max}) were read directly from the time-concentration profile of EC-18 in the plasma.

3. Results and Discussion

3.1. Mass spectrometry and Chromatography

The chemical structures of EC-18 and EC-18-d3 (i.e., the IS) are depicted in Fig. 1. The m/z values of EC-18 and IS were detected at 635.4→ 355.4 and 638.4→338.4, respectively (Fig. 1). An optimized chromatographic run time of 7 min per sample yielded symmetrical peaks for both analytes with an adequate separation between them and from other interfering peaks (Fig. 2). Based on these observations, the chromatographic conditions that resulted in retention times of 5.2 min for EC-18 and IS were selected. This spectrometric and chromatographic conditions were used in subsequent studies

3.2. Specificity, lower limit of quantification and linearity

EC-18 and IS were readily separated from the other peaks identified the double blank matrix under the LC–MS/MS conditions used (Fig. 2). Additionally, chromatograms, obtained from six different lots of blank analyses, indicated that no interfering peak was apparent in the vicinity of the analyte peaks (Fig. 2 and Table 1), suggesting that the assay has adequate specificity for quantitating EC-18 and IS in rat and mouse plasma samples. At the lower limit of quantification (LLOQ) level (i.e., 50 ng/mL) for EC-18, the precision (CV) of the peak area was 6.3 and 7.1% in rat and mouse plasma,

respectively (Table 1), with the signal to noise ration of at least 5 at LLOQ. The linearity of EC-18 in rat/mouse plasma samples, as estimated from five separate runs of calibration curves, was adequate, as evidenced by a correlation coefficient of at least 0.999 (Table 2) in the range of concentration of EC-18 from 50 to 10000 ng/mL.

3.3. Accuracy, precision, and sample dilution

Quality control (QC) samples, consisting of four concentration levels of EC-18 at 50, 150, 1000, and 8000 ng/mL in the rat and mouse plasma, were analyzed in six replicates to determine intra-day accuracy (RE) and CV. In the QC samples for the rat and mouse, the RE for EC-18 ranged from –4.4 to 10.4% and from –2.8 to 4.8% respectively, and the CV ranged from 5.5 to 10.1% and from 5.8 to 9.9%, respectively (Table 3). In this study, the inter-day validation parameters also were estimated using six QC replicates at the four concentration levels on five different days. The RE and CV for EC-18 ranged from –4.0 to 12.0% and from 5.3 to 9.7% in the rat plasma and ranged from –4.0 to 2.0% and from 6.4 to 13.9% in the mouse plasma, respectively (Table 3).

In some pharmacokinetic studies, a concentration exceeding the upper limit of quantification may occur, and the diluting of the sample with blank matrices may become necessary. To determine the feasibility of such a dilution, a set of plasma samples was prepared that contained an EC-18 concentration at 80000 ng/mL (i.e., 8 times the upper limit of the assay) and

diluted tenfold with blank plasma. The calculated concentration was found to be 8110 ng/mL with a CV of 2.4% and 8140 ng/ml with a CV of 7.4% in samples from rats and mice, respectively (Table 3), suggesting that plasma samples with concentration exceeding the upper limit of the assay may be diluted prior to the analysis.

3. 4. Matrix effect and recovery

In this study, the matrix effect and recovery of the assay were also estimated. QC plasma samples containing EC-18 (150, 1000, and 8000 ng/mL) were prepared using six different rats and mice, the samples were processed according to the procedure and the mean peak areas of the analytes determined. This absolute matrix effect for EC-18 and IS ranged from 87.6 to 89.0% and from 87.7 to 91.9% in rat QC samples and ranged from 77.9 to 83.4% and from 78.7 to 82.5% in mouse QC samples, respectively (Table 4), indicating that the matrix (i.e., plasma) suppresses the ionization of EC-18 [15]. In addition, the relative matrix effect was estimated by directly comparing the peak areas corresponding to EC-18 and IS that had been added to post-extracted blank plasma (from six different rats/mouse) (set 2). The CV for the peak area for EC-18 and IS in set 2 ranged from 2.9 to 4.1% and from 3.2 to 3.5% in the case of the rat QC samples and ranged from 3.4 to 5.4% and from 3.4 to 3.7% in mouse QC samples, respectively (Table 4). The CV for EC-18 and IS in set 1 (i.e., methanolic solution containing the analyte) ranged from 3.4 to 6.5% and from 2.7 to 4.3% for the validation study in rat

plasma samples and ranged from 2.9 to 3.4% and from 2.8 to 3.3% for the validation study for the mouse plasma samples, respectively (Table 4). These observations indicate that the variabilities of the analytes for set 1 (i.e., methanolic solution of the analytes) and set 2 (i.e., analytes added to post-extracted blank plasma) were comparable. The CV for the ratio of the peak areas of EC-18 to that of IS ranged from 0.7 to 1.6% and from 0.2 to 2.8% for the set 2 sample from the rat and the mouse, respectively, and from 1.4 to 5.8% and from 0.5 to 2.5%, respectively, for set 1 samples. Collectively, these observations indicate that the relative matrix effects for EC-18 and IS are negligible in the current procedure. On the other hand, the overall recovery of EC-18 and IS ranged from 41.0 to 53.2% and from 72.2 to 80.1% in rat QC samples and from 33.0 to 43.0% and from 63.7 to 65.8% in mouse QC samples, respectively (Table 4). Despite the fact that the recovery of EC-18 was comparatively low, the variability in the recovery was small (i.e., less than 12.2%) for the current method. In addition, the precision of the assay was consistently less than 10%. Considering the fact that the assay is straightforward (i.e., the plasma is extracted with MeOH) and rapid (i.e., theoretically up to 180 runs in a day can be performed), the present assay may be practically useful, especially in pharmacokinetic studies.

3.5. Stability

The stability of EC-18 in the stock solution at a concentration of 500 ng/mL was studied for storage at room temperature for 6 h, in refrigerated

conditions (4°C) for 24 h / 2 weeks, and in two frozen conditions (–20°C and –80°C) for 2 weeks with six replicates each (Table 5). The concentration of the stored sample was found to be 100.9% at room temperature for 6 hours. The concentrations of the stored samples were found to be 98.7 and 98.3% in refrigerated conditions (4°C) for 24 hours and 2 weeks, respectively. After maintaining frozen conditions for 2 weeks at –20 and –80°C, the sample concentrations were found to be 97.4 and 99.6% of the initial concentration, respectively. Collectively, the stability of the stock solution was deemed to be adequate for the storage conditions listed.

When QC samples, consisting of three concentration levels at 150, 1000 and 8000 ng/mL, were allowed to stand at room temperature for 24 h, the calculated concentrations were 150, 999 and 7920 ng/mL and 149, 1040 and 8140 ng/mL in rat and mouse QC samples, respectively (Table 6). Similarly, a post-preparative stability study indicated that the concentrations found in the samples are 97.1, 93.1 and 97.7% and 95.3, 104.7 and 98.7% of the theoretical values in rat and mouse QC samples, respectively (Table 6). For the case of a repeated freeze-thaw process, three cycles of freeze-thawing had a minor effect on the stability of EC-18 as evidenced by the fact that three concentrations of the QC samples were 88.7, 90.2 and 92.5%, and 89.8, 92.5 and 93.5% in rat and mouse QC samples, respectively (Table 6). The long-term storage of rat plasma samples at –80°C appeared to be adequate in terms of stability, since the estimated concentration was close to the theoretical values (i.e., differences of –5.1, –7.4 and –2.3% and –5.6, –6.8 and –1.3% in

rat and mouse QC samples, respectively, Table 6). Therefore, these observations indicate that EC-18 is stable under typical conditions and that the processing/storage conditions have no significant effect on the estimation of EC-18 concentrations in rat and mouse plasma samples.

3.6. Applicability in pharmacokinetic studies

To determine whether the current assay may be applied to a pharmacokinetic study of EC-18 in small animals such as the rat and mouse, the monoacetyldiglyeride was administered to rats/mice via two typical routes and the concentration in the plasma determined. The mean concentration time profile for EC-18 is shown in Fig. 3 for intravenous administration study at a dose of 1 mg/kg in rats and 5 mg/kg in mice. The mean concentration time profile for EC-18 is shown in Fig. 3. The concentrations of EC-18 were readily measurable in all plasma samples in both animal models after the intravenous administration, suggesting that the current assay is adequate for determining the distributive and eliminatory characteristics of EC-18 in the body. The calculated pharmacokinetic parameters, including $T_{1/2}$, Cl, AUC_{inf}, MRT and V_{ss}, are listed in Table 7. In general, the compound appeared to have a limited distribution space while being cleared rapidly in the small animal models.

In the case of the oral administration study at a dose of 2000 mg/kg in rats and mice, however, the exposure of EC-18 was very low in mice (AUC_{inf} was 4.23 h · μg/mL) and was generally not measurable, except for a

few time-points in rats (Fig. 3, Table 7). Assuming that the extent of absorption of 0.034% in mice is applicable to rats, the concentration predicted by physiologically based pharmacokinetic modeling (Supplementary Material Fig. S1) in the vicinity of C_{max} would be approximately 1.09 μg/mL. Furthermore, the drug concentration should have been detected (LLOQ of the assay of 50 ng/mL) for up to 8 h after its administration (Supplementary Material Fig. S1) if the pharmacokinetics from mice could be scaled to rats. Collectively, these observations suggest that a species difference exists in intestinal absorption, consistent with literature information on the absorptive/eliminatory properties of other glycerides.

4. Discussion

An LC–MS/MS procedure for determining EC-18 levels in rat and mouse plasma samples was developed and validated in terms of selectivity, linearity, accuracy, precision, matrix effects, recovery, and stability. The developed method involves a simple, straightforward sample preparation and a rapid LC run-time (7 min), while having an acceptable sensitivity/reliability for pharmacokinetic studies involving EC-18. Therefore, the developed assay in this study may be useful in pharmacokinetic studies dealing with EC-18 in animal models.

5. References

[1] F. Oshita, T. Tamura, H. Okamoto, T. Miya, A. Kojima, Y. Ohe, Y. Sasaki, K. Eguchi, T. Shinkai, N. Saijo, The frequency and management of infectious episodes and sepsis in small cell lung cancer patients receiving intensive chemotherapy with granulocytecolony stimulating factor, Jpn. J. Clin. Oncol. 21(5) (1991) 353-359.

[2] T. Cerny, A. Pedrazzini, R. Joss, K. Brunner, Unexpected high toxicity in a phase II study of teniposide (VM-26) in elderly patients with untreated small cell lung cancer (SCLC), Eur. J. Cancer Clin. Oncol. 24(11) (1988) 1791-1794.

[3] F. Oshita, T. Kurata, T. Kasai, M. Fukuda, N. Yamamoto, Y. Ohe, T. Tamura, K. Eguchi, T. Shinkai, N. Saijo, Prospective Evaluation of the Feasibility of Cisplatin-based Chemotherapy for Elderly Lung Cancer Patients with Normal Organ Functions, Jpn. J. Cancer Res. 86(12) (1995) 1198-1202.

[4] M. Kondo, F. Oshita, Y. Kato, K. Yamada, I. Nomura, K. Noda, Early monocytopenia after chemotherapy as a risk factor for neutropenia, Am. J. Clin. Oncol. 22(1) (1999) 103-105.

[5] H.O. Yang, S.H. Kim, S.-H. Cho, M.-G. Kim, J.-Y. Seo, J.-S. Park, G.-J. Jhon, S.-Y. Han, Purification and structural determination of hematopoietic stem cell-stimulating monoacetyldiglycerides from Cervus nippon (deer antler), Chem. Pharm. Bull. 52(7) (2004) 874-878.

[6] T.-S. Lee, J.-S. Yook, C.-H. Yoo, C.-M. Lee, E.-k. Kim, J.-C. Lee, Method for preparing monoacetyglycerols and esters thereof, https://www.google.ch/patents/US20150266803, 2014, (accessed 2016.10.03)

[7] M.-H. Kim, H.M. Chang, T.W. Kim, S.K. Lee, J.-S. Park, Y.-H. Kim, T.Y. Lee, S.J. Jang, C.-W. Suh, T.-S. Lee, EC-18, a synthetic monoacetyldiacylglyceride, inhibits hematogenous metastasis of KIGB-5 biliary cancer cell in hamster model, J. Korean Med. Sci. 24(3) (2009) 474-480.

[8] J. Jeong, Y.-J. Kim, S.Y. Yoon, Y.-J. Kim, J.H. Kim, K.-Y. Sohn, H.-J. Kim, Y.-H. Han, S. Chong, J.W. Kim, PLAG (1-Palmitoyl-2-Linoleoyl-3-Acetyl-rac-Glycerol) modulates eosinophil chemotaxis by regulating CCL26 expression from epithelial cells, PloS one 11(3) (2016) e0151758.

[9] I.-S. Shin, K.-S. Ahn, N.-R. Shin, H.-J. Lee, H.W. Ryu, J.W. Kim, K.-Y. Sohn, H.J. Kim, Y.-H. Han, S.-R. Oh, Protective effect of EC-18, a synthetic monoacetyldiglyceride on lung inflammation in a murine model induced by cigarette smoke and lipopolysaccharide, Int. Immunopharmacol. 30 (2016) 62-68.

[10] A.J. Humberstone, W.N. Charman, Lipid-based vehicles for the oral delivery of poorly water soluble drugs, Adv. Drug Delivery Rev. 25(1) (1997) 103-128.

[11] L.M. Berry, L. Wollenberg, Z. Zhao, Esterase activities in the blood, liver and intestine of several preclinical species and humans, Drug Metab. Lett. 3(2) (2009) 70-77.

[12] A. Dahan, A. Beig, D. Lindley, J.M. Miller, The solubility–permeability interplay and oral drug formulation design: Two heads are better than one, Adv. Drug Delivery Rev. 101 (2016) 99-107.

[13] O.M. Feeney, M.F. Crum, C.L. McEvoy, N.L. Trevaskis, H.D. Williams, C.W. Pouton, W.N. Charman, C.A. Bergström, C.J. Porter, 50years of oral lipid-based formulations: Provenance, progress and future perspectives, Adv. Drug Delivery Rev. 101 (2016) 167-194.

[14] T.A. Baillie, R.A. Halpin, B.K. Matuszewski, L.A. Geer, C.M. Chavez-Eng, D. Dean, M. Braun, G. Doss, A. Jones, T. Marks, Mechanistic studies on the reversible metabolism of rofecoxib to 5-hydroxyrofecoxib in the rat: evidence for transient ring opening of a substituted 2-furanone derivative using stable isotope-labeling techniques, Drug Metab. Dispos. 29(12) (2001) 1614-1628.

[15] B. Matuszewski, M. Constanzer, C. Chavez-Eng, Strategies for the assessment of matrix effect in quantitative bioanalytical methods based on HPLC-MS/MS, Anal. Chem. 75(13) (2003) 3019-3030.

[16] M. Gibaldi, D. Perrier, Pharmacokinetics, Second Edition, Revised and Expanded. Marcel Dekker, Inc., New York, 1982, pp. 409-416.

[17] H. Leskinen, J.P. Suomela, H. Kallio, Quantification of triacylglycerol regioisomers in oils and fat using different mass spectrometric and liquid chromatographic methods, Rapid Commun. Mass Spectrom. 21(14) (2007) 2361-2373.

[18] A.A. Zoerner, S. Batkai, M.-T. Suchy, F.-M. Gutzki, S. Engeli, J. Jordan,

D. Tsikas, Simultaneous UPLC–MS/MS quantification of the endocannabinoids 2-arachidonoyl glycerol (2AG), 1-arachidonoyl glycerol (1AG), and anandamide in human plasma: Minimization of matrix-effects, 2AG/1AG isomerization and degradation by toluene solvent extraction, J. Chromatogr. B 883 (2012) 161-171.

[19] B. K. Matuszewski, M. L. Constanzer, C. M. Chavez-Eng, Strategies for the assessment of matrix effect in quantitative bioanalytical methods based on HPLC-MS/MS. Anal. Chem. 75(13) (2003) 3019-3030.

[20] J. H. Lee, Y. A. Woo, I. C. Hwang, C. Y. Kim, D. D. Kim, C. K. Shim, S. J. Chung, Quantification of CKD-501, lobeglitazone, in rat plasma using a liquid-chromatography/tandem mass spectrometry method and its applications to pharmacokinetic studies. J. Pharm. Biomed. Anal., 50(5) (2009) 872-877.

[21] J. H. Lee, Y. J. Chae, K. R. Lee, S. H. Ahn, J. W. Seo, Q. R. Jin, Y. A. Woo, G. W. Lee, S. C. Cho, S. W. Kwon, D. H. Park, Development of a LC–MS method for quantification of FK-3000 and its application to in vivo pharmacokinetic study in drug development. J. Pharm. Biomed. Anal., 70 (2012) 587-591.

[22] FDA, Draft guidance for industry: bioanalytical method validation, US Department of Health and Human Services, US FDA (2013).

Table 1

Specificity of EC-18 measurements in rats and mice plasma

Matrix lot.	Response (Peak area)							
	Rats plasma				Mice plasma			
	Blank[a)]	Zero blank[b)]	LLOQ (50 ng/mL)	HQC (8000 ng/mL)	Blank[a)]	Zero blank[b)]	LLOQ (50 ng/mL)	HQC (8000 ng/mL)
1	0.0	0.0	82.6	14800	0.0	0.0	77.0	10500
2	0.0	0.0	98.2	13600	0.0	0.0	72.3	11000
3	0.0	0.0	97.8	17300	0.0	0.0	66.5	12900
4	0.0	0.0	89.0	16600	0.0	0.0	64.3	11300
5	0.0	0.0	91.2	16900	0.0	0.0	69.4	10500
6	0.0	0.0	92.0	16500	0.0	0.0	75.6	11000
Mean	0.0	0.0	91.8	16000	0.0	0.0	70.8	11200
CV (%)[c)]	0.0	0.0	6.3	9.0	0.0	0.0	7.1	7.9

a) Sample containing no analyte or IS, was extracted and analyzed.

b) Samole containing only IS, was extracted and analyzed.

c) CV (%) = standard deviation / mean × 100.

Table 2

Calibration curves of EC-18 in rats and mice plasma

Run	Rats plasma			Mice plasma		
	Slope	Intercept	*R*	Slope	Intercept	*R*
1	0.000979	–0.0390	0.999	0.000443	0.0120	0.999
2	0.000817	–0.0325	0.998	0.000505	–0.00547	0.999
3	0.000885	–0.0309	0.999	0.000432	0.00988	0.999
4	0.000891	–0.0249	0.999	0.000525	–0.00880	0.999
5	0.000926	–0.00446	0.999	0.000520	0.00402	0.998
Mean	0.000900	–0.0264	0.999	0.000485	0.00233	0.999
CV (%)[a)]	6.8	- b)	-	8.9	- b)	-

a) CV (%) = standard deviation / mean × 100.

b) Not applicable.

Table 3

Quality control sample of EC-18 in rats and mice plasma

Batch	Theoretical concentration (ng/mL)				
	LLOQ	LQC	MQC	HQC	HQC
	50	150	1000	8000	8000[a)]
Rats plasma					
(A) Intraday accuracy and precision (n=6)					
Mean estimated concentration	55.2	143	1010	8000	8110
CV (%)[b)]	10.1	7.0	6.4	5.5	2.4
RE (%)[c)]	10.4	–4.4	1.0	0.0	1.4
(B) Inter-day accuracy and precision (n=30)					
Mean estimated concentration	56.0	144	972	7930	
CV (%)	9.7	5.3	9.0	6.1	
RE (%)	12.0	–4.0	–2.8	–0.9	
Mice plasma					
(A) Intraday *accuracy and precision (n=6)*					
Mean estimated concentration	52.0	146	1040	8380	8140
CV (%)[b)]	9.9	8.1	8.5	5.8	7.4
RE (%)[c)]	3.9	–2.8	4.0	4.8	1.8
(B) Inter-day accuracy and precision (n=30)					
Mean estimated concentration	48.0	146	1020	8130	
CV (%)	13.9	7.1	8.5	6.4	
RE (%)	−4.0	–2.9	2.0	1.6	

a) Analyzed after a tenfold dilution with blank rat plasma (i.e., 80000 → 8000 ng/mL).

b) CV (%) = standard deviation for the concentration / mean concentration × 100.

c) RE (%) = (calculated concentration – theoretical concentration)/ theoretical concentration × 100.

Table 4

Matrix effect, recovery, and precision (CV, %) for EC-18 and EC-18-d3 (internal standard) in six different lots of rats and mice plasma

Nominal Concentration (ng/mL)	Absolute Matrix effect[a)]		Recovery[b)](%)		Precision[c)] (CV, %)					
					EC-18		IS		EC-18/IS	
	EC-18	IS	EC-18	IS	Set 1	Set 2	Set 1	Set 2	Set 1	Set 2
Rats plasma										
150	89.0	91.9	41.0	72.2	6.5	2.9	2.7	3.2	5.8	0.7
1000	88.0	89.4	48.6	73.9	4.7	4.1	3.1	3.5	4.6	1.3
8000	87.6	87.7	53.2	80.1	3.4	3.2	4.3	3.4	1.4	1.6
Mice plasma										
150	83.4	81.9	33.0	63.7	3.1	5.4	3.3	3.7	0.5	2.2
1000	77.9	78.7	37.8	65.8	3.4	3.8	3.0	3.7	2.5	0.2
8000	82.3	82.5	43.0	64.6	2.9	3.4	2.8	3.4	0.6	2.8

a) Absolute matrix effect expressed as the ratio of the mean peak area of an analyte added post-extraction (set 2) to the mean peak area of the same analyte standards (set 1) multiplied by 100.

b) Recovery, calculated as the ratio of the mean peak area of an analyte added before extraction to the mean peak area of an analyte spiked post-extraction (set 2) multiplied by 100.

c) Precision of determination of peak areas of EC-18 and IS, and peak area ratios (EC-18/IS) in set 1 and 2 as the measure of relative matrix effect.

Table 5

Stability of EC-18 in stock solutions

Batch	Response (Peak area) [a]					
	Initial (0 h)	Room temp. (6 h)	4°C (24 h)	4°C (2 weeks)	-20°C (2 weeks)	-80°C (2 weeks)
Number of samples	3	3	3	3	3	3
Mean response	2310	2330	2280	2270	2250	2300
CV (%)	6.0	6.0	3.4	6.8	3.9	7.5
Relative conc. (%) [b]	100.0	100.8	98.7	98.3	97.4	99.6

a) Stock solutions were diluted to 500 ng/mL prior to analysis.

b) Relative concentration (%) obtained from the measured value divided by the initial value.

Table 6

Stability of quality control samples

Batch	Rats plasma			Mice plasma		
	Theoretical concentration (ng/mL)			Theoretical concentration (ng/mL)		
	150	1000	8000	150	1000	8000
(A) Benchtop stability at room temperature for 24 h (n=3)						
Mean estimated concentration	150	999	7920	149	1040	8140
CV (%)[a)]	0.4	2.9	6.5	3.0	3.5	4.4
RE (%)[b)]	−0.2	–0.1	–1.0	–0.9	4.0	1.8
(B) Post-preparative stability at 4°C for 3 days (n=3)						
Mean estimated concentration	146	931	7820	143	1050	7890
CV (%)	7.3	1.6	6.0	5.3	7.2	4.7
RE (%)	−2.9	–6.9	–2.3	–4.7	4.7	–1.4
(C) Freeze–thaw stability (3 cycles) (n=3)						
Mean estimated concentration	133	902	7400	135	925	7480
CV (%)	8.5	2.0	2.6	2.4	2.8	2.5
RE (%)	−11.3	–9.8	–7.5	–10.2	–7.5	–6.5
(D) Long-term stability for 2 weeks (n=3)						
Mean estimated concentration	142	926	7820	142	932	7900
CV (%)	8.9	4.2	4.0	6.7	7.1	3.8
RE (%)	−5.1	–7.4	–2.3	–5.6	–6.8	–1.3

a) CV (%) = standard deviation of the concentration / mean concentration × 100.

b) RE (%) = (calculated concentration – theoretical concentration)/ theoretical concentration × 100.

Table 7

Pharmacokinetic parameters of EC-18 in rats and mice (mean ± standard deviation)

Pharmacokinetic parameters		rats	mice	
		iv injection	iv injection	oral administration
$T_{1/2}$	*h*	1.25 ± 0.06	1.17	
CL	*mL/h/kg*	32.1 ± 3.3	161	
AUC_{inf}	*h · μg/mL*	31.3 ± 3.1	31.1	4.23
MRT	*h*	1.78 ± 0.31	1.32	
V_{ss}	*mL/kg*	58.0 ± 16.2	212	
T_{max}	*h*			4.0
C_{max}	*μg/mL*			0.231

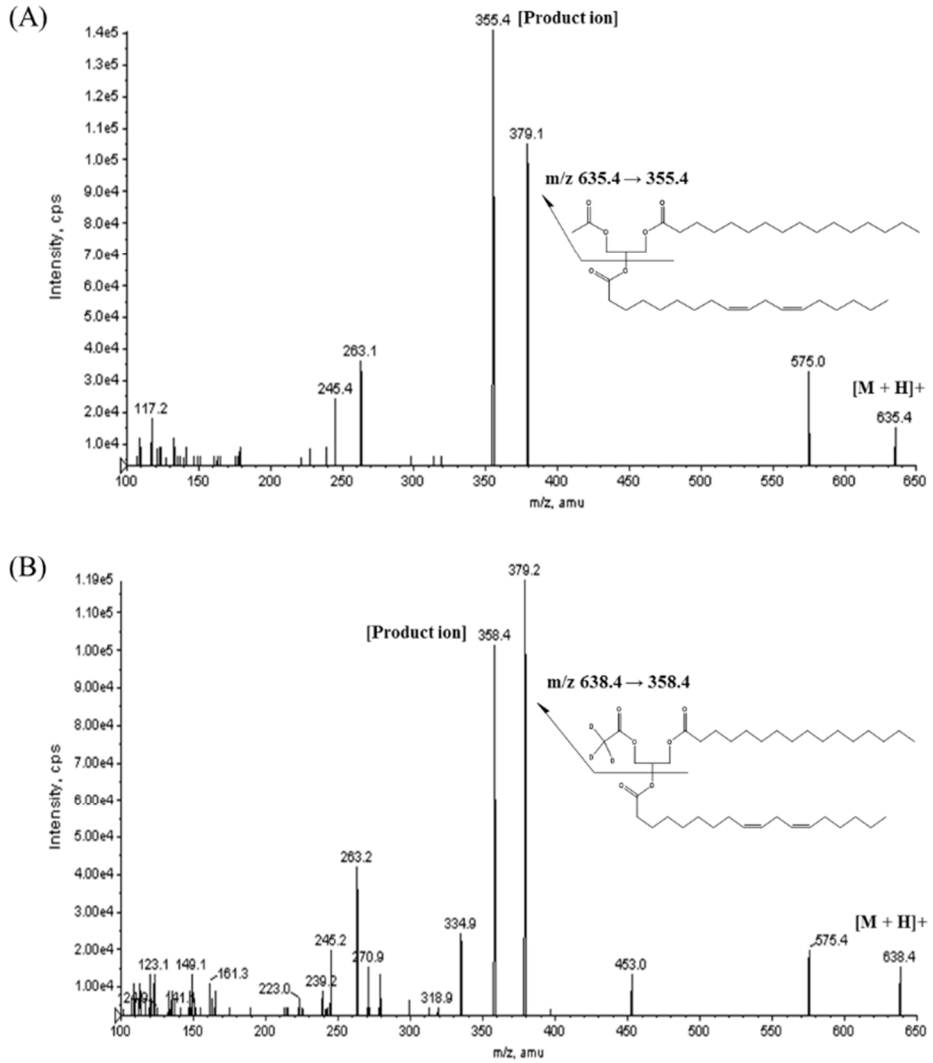

Fig. 1. The structures and product-ion scan spectra of (A) EC-18 and (B) EC-18-d3 (i.e., internal standard).

(A)

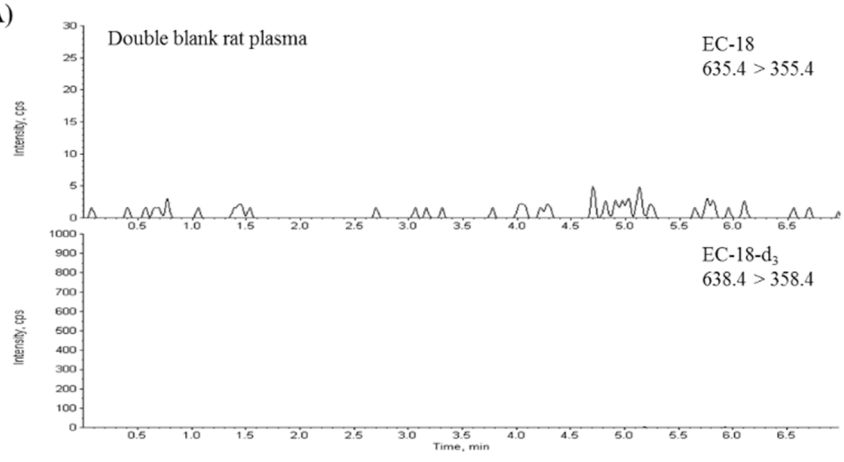
Double blank rat plasma
EC-18
635.4 > 355.4
EC-18-d3
638.4 > 358.4
Intensity, cps
Time, min

(B)

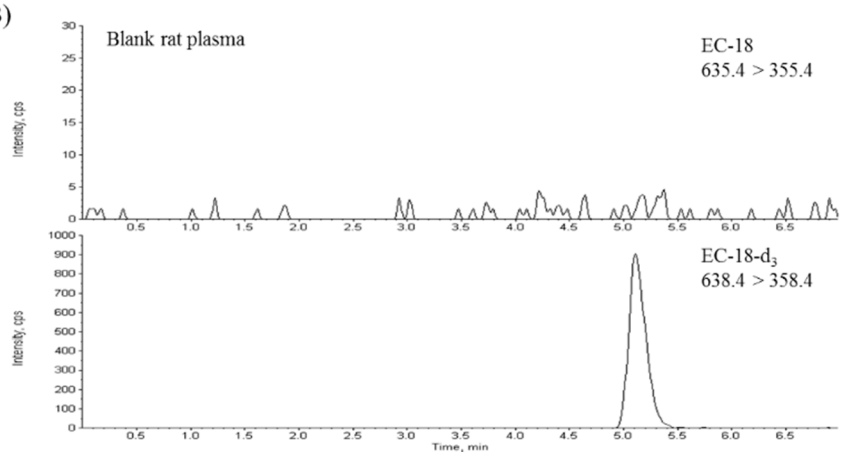
Blank rat plasma
EC-18
635.4 > 355.4
EC-18-d3
638.4 > 358.4
Intensity, cps
Time, min

(C)

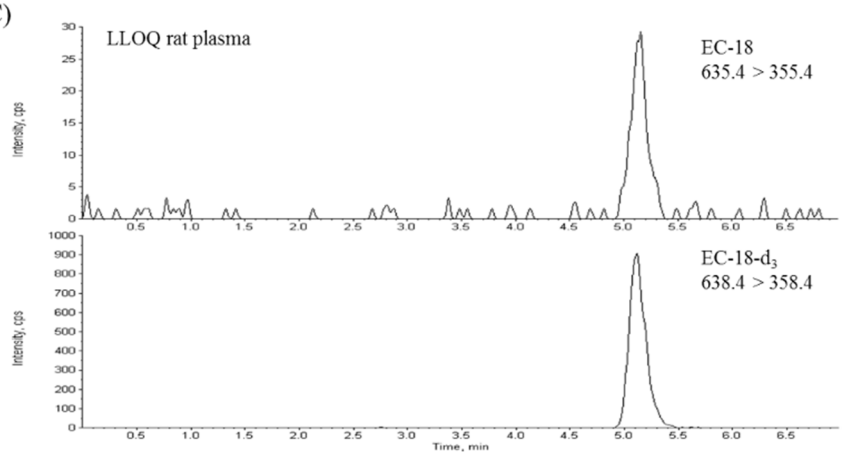
LLOQ rat plasma
EC-18
635.4 > 355.4
EC-18-d3
638.4 > 358.4
Intensity, cps
Time, min

(D)

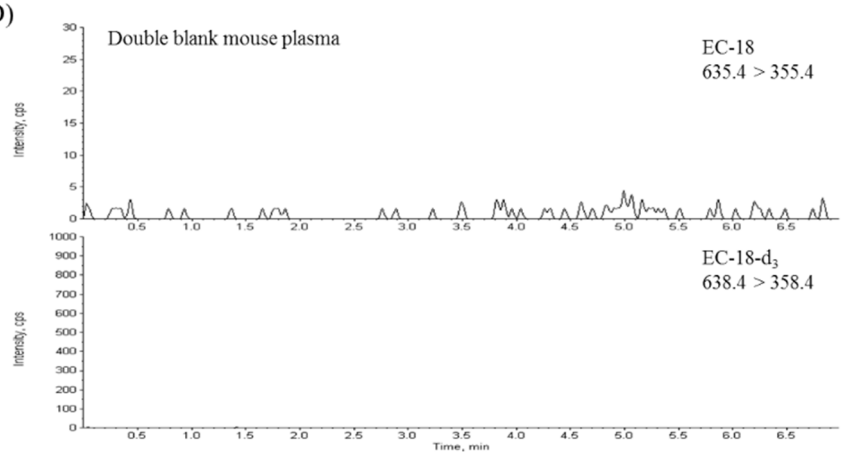
Double blank mouse plasma
EC-18
635.4 > 355.4
EC-18-d3
638.4 > 358.4
Intensity, cps
Time, min

(E)

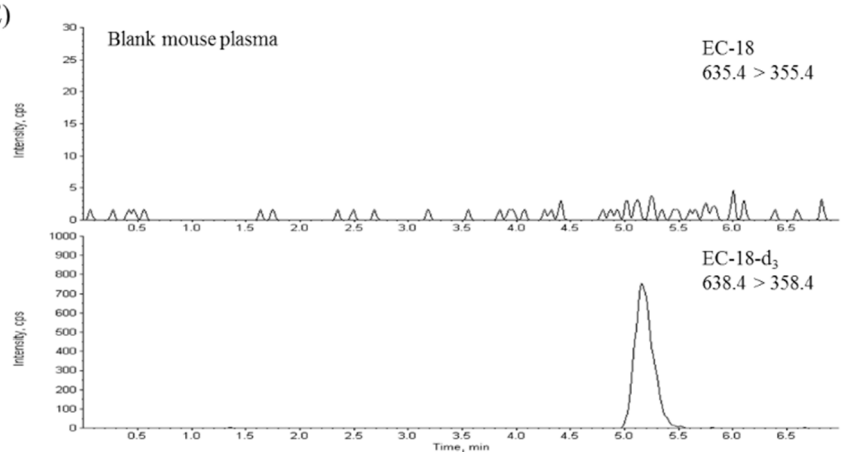
Blank mouse plasma
EC-18
635.4 > 355.4
EC-18-d3
638.4 > 358.4
Intensity, cps
Time, min

(F)

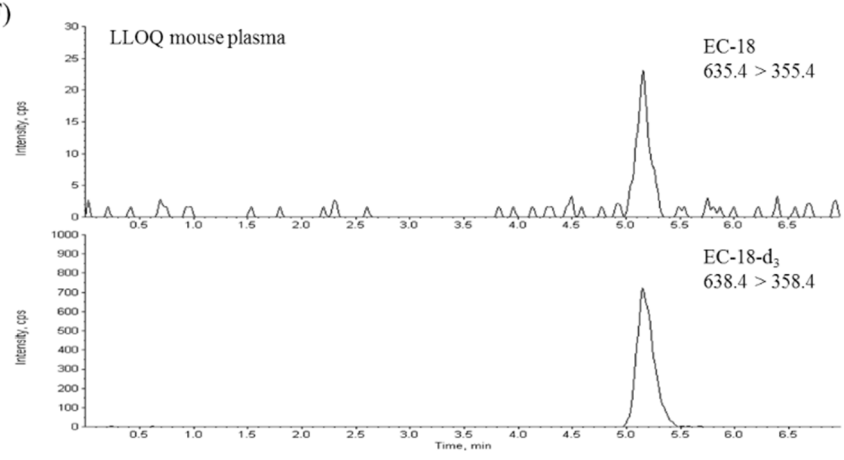
LLOQ mouse plasma
EC-18
635.4 > 355.4
EC-18-d3
638.4 > 358.4
Intensity, cps
Time, min

Fig. 2. Multiple reaction monitoring (MRM) chromatograms of: (A) double blank rat plasma, (B) rat plasma containing EC-18-d3 (IS, 200 ng/mL), (C) rat plasma containing EC-18 at LLOQ (50 ng/mL) and IS, (D) double blank mouse plasma, (E) mouse plasma containing EC-18-d3 (IS, 200 ng/mL), and (F) mouse plasma containing EC-18 at LLOQ (50 ng/mL) and IS.

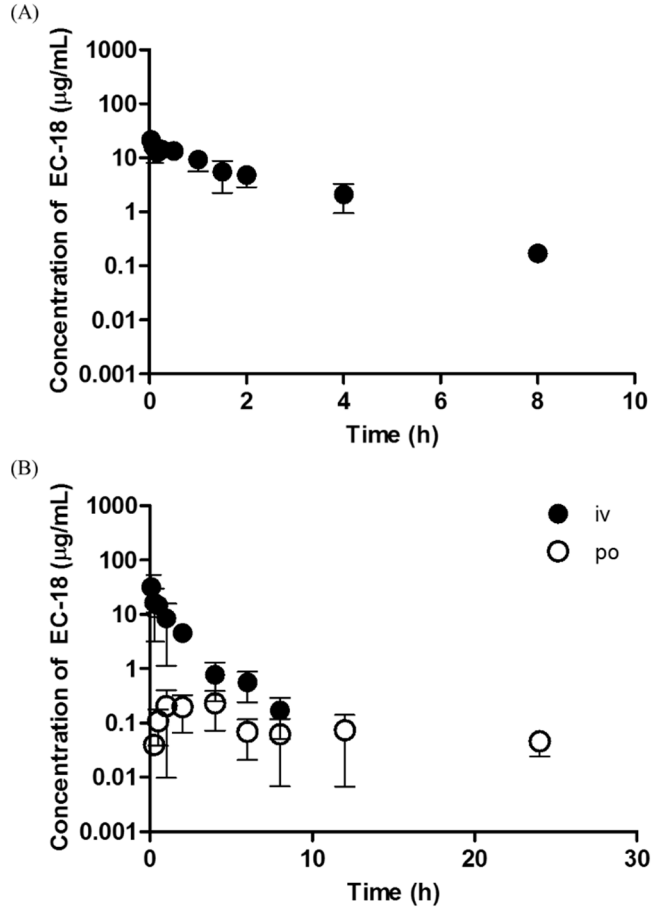

Fig. 3. The mean concentration time profile of EC-18. (A) Intravenous injection in rats (1 mg/kg), (B) intravenous injection (5 mg/mg) and ora l administration (2000 mg/kg) in mice. Each point represents the Mean ± standard deviation (n=3).

6. APPENDICES

6.1. APPENDIX A

In this study, we conducted a series of simulation studies for the estimation of the concentration profiles of EC-18 in the plasma of the mouse and rat. For pharmacokinetic calculation, Simcyp® software [1] version 15 Release 1 (Simcyp Limited, Sheffield, UK) was used. Since V_{ss} of EC-18 in rats and mice were low (i.e., 58.0 and 212 mL/kg, respectively), a minimal PBPK model without SAC (i.e., single adjusting compartment) was considered adequate for estimating the distribution kinetics of the compound [2] and the resulting equations for the model presented as described below :

For the systemic compartment;

$$V_{sys}\frac{C_{sys}}{dt} = Dose\ rate + Q_H \cdot \left(\frac{C_{LI}}{K_{p,LI}} - C_{sys}\right) - CL_{sys} \cdot C_{sys} \quad (S1)$$

For the portal vein compartment;

$$V_{PV}\frac{C_{PV}}{dt} = Q_{PV} \cdot (C_{sys} - C_{PV}) + k_a \cdot X_{GI} \quad (S2)$$

For the liver compartment;

$$V_{LI}\frac{C_{LI}}{dt} = Q_{HA} \cdot C_{sys} + Q_{PV} \cdot C_{PV} - Q_H \cdot \frac{C_{LI}}{K_{p,LI}} \quad (S3)$$

For the gastrointestinal compartment'

$$\frac{dX_{GI}}{dt} = -k_a \cdot X_{GI} \quad (S4)$$

where C_{sys}, C_{PV}, and C_{LI} are the concentration of drug in the systemic, portal vein, and liver compartment, respectively; V_{sys}, V_{PV}, and V_{LI} are the apparent volume of the systemic (i.e., $V_{ss} - V_{LI}$), portal vein, and liver compartment, respectively; Q_H, Q_{HA}, and Q_{PV} are the hepatic, hepatic artery, and portal blood flow, respectively; $K_{p,LI}$ is the liver-to-plasma concentration ratio (i.e., this value was arbitrarily set as unity); X_{GI} is the amount of drug in the gastrointestinal compartment; k_a is the absorption rate constant; CL_{sys} is the systemic clearance. When necessary, the V_{ss} and systemic clearance, calculated from moment analysis (Table 7), were also used.

In this study, the concentration-time profile after oral administration of EC-18 was available only in mice: Therefore, the concentration profile in rats was simulated under the assumption of linear pharmacokinetics for EC-18 and the first order kinetics in the intestinal absorption. The absorption rate constant k_a of the mouse, obtained from the data, was assumed to be identical to that in rats. In a preliminary study, *in silico* prediction of k_a was considered, although this approach resulted in unrealistic value for k_a in mice, probably because of the high lipophilicity of the glyceride thereby leading to unacceptable prediction (i.e., calculated log P, 11.14; MarvinSketch software, ChemAxon, Budapest, Hungary) (data not shown). Therefore, k_a and other pharmacokinetic variables were either obtained from Parameter Estimation Method built in Simcyp® software or consolidated from the observation as described above. The list of pharmacokinetic parameters used

in the calculation was summarized in Table S1. Based on the model and the parameters, the predicted concentration-time profile of EC-18 in the plasma after intravenous administration was reasonable for the both species (Fig. S1). In addition, the predicted profile of EC-18 was adequate in mice. Interestingly, however, the calculation predicted that the concentration in the rat plasma be above 50 ng/mL (i.e., LLOQ of the study) from time 0.11 to 24 h in rats when the oral dose was given (Fig. S1) if the pharmacokinetic assumption is valid. Therefore, these observations indicate that there is a species-difference in kinetics of intestinal absorption for EC-18. This aspect of EC-18 pharmacokinetics warrants further investigation.

Table S1

Summary of pharmacokinetic parameters for EC-18 used in the calculation for rats and mice

pharmacokinetic parameters		rats	mice
$K_{p,LI}$		1	
k_a	h^{-1}	0.075	
Q_{HA}	*mL/min*	1.28	0.614
Q_{PV}	*mL/min*	18.1	2.54
Q_H	*mL/min*	19.4	3.15
V_{LI}	*mL*	8.57	1.19

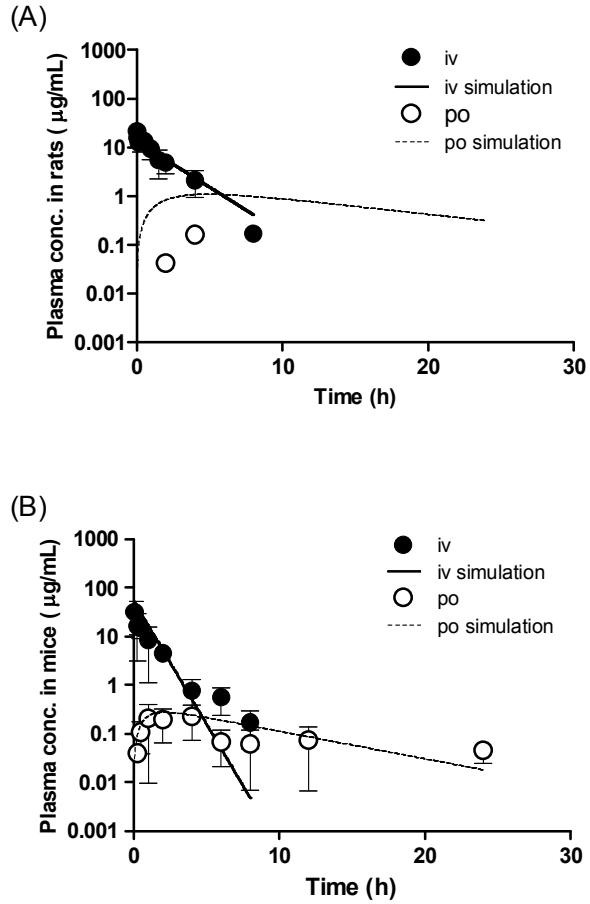

Fig. S1 Observed and predicted plasma concentration time profile of EC-18 after intravenous and oral administrations in rats (Panel A) and mice (Panel B). Intravenous injection in rats (1 mg/kg), intravenous injection (5 mg/kg) and oral administration (2000 mg/kg) in mice was given to animals (indicated as symbols in the Figure). The line in the figure represents the concentration calculated using pharmacokinetic models assuming the EC-18 administrations [i.e., intravenous injection in rats (1 mg/kg), intravenous injection (5 mg/kg) and oral administration (2000 mg/kg) in mice].

References

[1] M. Jamei, S. Marciniak, K. Feng, A. Barnett, G. Tucker, A. Rostami-Hodjegan, The Simcyp® population-based ADME simulator, Expert opinion on drug metabolism & toxicology 5(2) (2009) 211-223.

[2] Y. Cao, W.J. Jusko, Applications of minimal physiologically-based pharmacokinetic models, Journal of pharmacokinetics and pharmacodynamics 39(6) (2012) 711-723.

[3] M. Fujikawa, R. Ano, K. Nakao, R. Shimizu, M. Akamatsu, Relationships between structure and high-throughput screening permeability of diverse drugs with artificial membranes: application to prediction of Caco-2 cell permeability, Bioorganic & medicinal chemistry 13(15) (2005) 4721-4732.

6.2. APPENDIX B

In this study, we compared the mean peak area of QC samples to determine the effect of plasma volume. Samples were prepared followed method: preparation method of QC samples of set 1 was described in sections 2.4 and 2.5 of the main text. Briefly, 5 µL aliquot of an EC-18 solution was added to 45 µL of blank rat or mouse plasma. A 200 µL aliquot of IS solution (200 ng/mL in methanol containing 0.1% FA, v/v) was added to the sample. For set 2, samples were prepared by adding 5 µL aliquot of an EC-18 solution and 195 µL aliquot of IS solution (200 ng/mL in methanol containing 0.1% FA, v/v) to 50 µL of blank rat or mouse plasma. All samples were vortexed for 10 min and centrifuged at 16,100 g at 4°C for 10 min. A 5 µL aliquot was injected onto the LC-MS/MS system for the analysis of EC-18.

The mean peak areas of LLOQ in set 1 and set 2 were 91.8 and 88.8, and those of HQC were 16000 and 15300 in the rat plasma, respectively. For the case of the mouse plasma, the peak areas of LLOQ and HQC in set 1 and set 2 were 70.8, 64.9, and 11200, 10600, respectively. This result indicate that small difference in the sample composition led did not cause any statistical difference when analyzed by unpaired t-test for both rat/mouse plasma, and the difference in the response of the two sets may be attributed to the slight difference in the

matrix.

Matrix lot.	Response (Peak area)							
	Rat plasma				Mouse plasma			
	Set 1		Set 2		Set 1		Set 2	
	LLOQ	HQC	LLOQ	HQC	LLOQ	HQC	LLOQ	HQC
1	82.6	14800	85.9	13300	77.0	10500	70.1	10600
2	98.2	13600	93.3	14400	72.3	11000	57.8	9680
3	97.8	17300	93.9	15900	66.5	12900	70.5	11900
4	89.0	16600	81.9	16300	64.3	11300	64.9	10100
5	91.2	16900	86.6	16900	69.4	10500	57.6	11000
6	92.0	16500	91.1	14700	75.6	11000	68.8	10600
Mean	91.8	16000	88.8	15300	70.8	11200	64.9	10600
sd	5.8	1435	4.7	1347	5.0	890	6.0	766
CV (%)[c)]	6.3	9.0	5.3	8.8	7.1	7.9	9.2	7.2

Set 1, 45 µl plasma + 5 µl stock(10x) + 200 µl MeOH (0.1% FA, v/v))

Set 2, 50 µl plasma + 5 µl stock(10x) + 195 µl MeOH (0.1% FA, v/v))

6.3. APPENDIX C

In this study, we compared the mean peak area of QC samples to determine the effect of extraction medium. Method of preparation for QC samples was described in the sections 2.4 and 2.5 of the main text. Briefly, 5 μL (in methanol or acetonitrile containing 0.1% FA, v/v) aliquot of an EC-18 solution was added to 45 μL of blank rat or mouse plasma. A 200 μL aliquot of IS solution (200 ng/mL in methanol or acetonitrile containing 0.1% FA, v/v) was added to the sample. All samples were vortexed for 10 min and centrifuged at 16,100 g at 4°C for 10 min. A 5 μL aliquot was injected onto the LC-MS/MS system for the analysis of EC-18.

In rat plasma, the mean peak areas of LLOQ and HQC were 91.8 and 16000 with methanol precipitation method, while the values were 89.7 and 16700 with acetonitrile precipitation method, respectively. In mouse plasma, those were 70.8 and 11200 with methanol precipitation method, and 72.0 and 10600 with acetonitrile precipitation method, respectively. These results indicate that deproteination medium such as methanol or acetonitrile did not render any statistical difference (i.e., unpaired t-test) in both rat/mouse plasma samples.

Matrix lot.	Response (Peak area)							
	Rats plasma				Mice plasma			
	Methanol		Acetonitrile		Methanol		Acetonitrile	
	LLOQ	HQC	LLOQ	HQC	LLOQ	HQC	LLOQ	HQC
1	82.6	14800	80.9	17500	77.0	10500	70.1	10300
2	98.2	13600	99.2	15400	72.3	11000	78.8	9900
3	97.8	17300	93.9	15700	66.5	12900	79.1	10400
4	89.0	16600	88.1	19900	64.3	11300	61.1	11000
5	91.2	16900	82.1	15500	69.4	10500	69.4	9200
6	92.0	16500	93.8	16200	75.6	11000	73.3	12800
Mean	91.8	16000	89.7	16700	70.8	11200	72.0	10600
SD	5.8	1400	7.2	1700	5.0	900	6.8	1200
CV (%)	6.3	9.0	8.1	10.5	7.1	7.9	9.4	11.6

7. 국문초록

EC-18 (1-palmitoyl-2-linoleoyl-3-acetyl-rac-glycerol)은 록피드®의 유효성분으로서, 특히 백혈수 감소증에 의한 염증증상을 조절하는데 유용한 것으로 보고되어 있다. 한국에서는 건강기능식품으로 허가를 받았지만, 열성 호중구 감소증을 보이는 진행성 유방암 환자를 대상으로 화학요법에 의한 호중구 감소증에 대한 임상 2상 시험을 진행중이다. 이 연구의 목적은 랫드와 마우스의 혈장에서 EC-18에 대한 빠르고, 민감한 분석방법을 개발하고 이를 약물동태학 연구에 적용하는 것이었다. 메탄올을 이용하요 랫드와 마우스의 혈장에서 EC-18을 추출하고 이를 LC-MS/MS에 주입하여 분석을 하였다. 검체와 EC-18-d3 (내부표준품)의 MRM 값은 각각 635.4→355.4, 638.4→338.4이었다. 두 종류의 혈장에서 최소정량한계는 50 ng/mL이었으며, 검량선의 수용 가능 직선성은 50 ~ 10000 ng/mL ($r > 0.999$)에서 확인하였다. 정확도, 정밀도, 희석효과, 회수율, 매트릭스 효과, 안정성과 같은 밸리데이션 파라미터는 모두 밸리데이션 가이드라인의 수용 범위 안에 들었으며, 이는 실험한 농도범위에서의 EC-18에 대한 분석 평가가 적절하였음을 말해주었다. 이에, 랫드에 1 mg/kg, 마우스에 5 mg/kg의 양으로 정맥주사를 하여 8시간 동안 실험하고, 마우스에 2000 mg/kg의

양으로 경구 투여하여 24시간동안의 혈장내 EC-18의 농도를 측정하였다. 그 결과 개발한 분석 방법은 두 동물 모델의 EC-18에 대한 약물동태학 실험을 하는데 적합한 것을 확인할 수 있었다.

주요어: EC-18; 1-palmitoyl-2-linoleoyl-3-acetyl-rac-glycerol; 약물동태학; LC-MS/MS 분석

학번: 2010-21709